Improving outcomes of minocycline treatment in severe infections caused by *Acinetobacter baumannii*

A Dissertation Presented to the

Faculty of the Department of Pharmacological and Pharmaceutical Sciences

College of Pharmacy, University of Houston

In Partial Fulfillment of

the Requirements for the Degree of

Doctor of Philosophy

By

Jian Zhou

July 2017

Improving outcomes of minocycline treatment in severe infections caused by *Acinetobacter baumannii*

Jian Zhou

Approved By:

Vincent Tam, Pharm.D. (Advisor)
University of Houston

Adriana E. Rosato, Ph.D.
The Methodist Hospital

Diana S-L Chow, Ph.D.
University of Houston

Song Gao, Ph.D.
University of Houston

Truc T. Tran, Pharm.D.
University of Texas

Lamar Pritchard, Ph.D.
Dean, College of Pharmacy

ACKNOWLEDGEMENTS

Firstly, I would like to express my sincere gratitude to my advisor Dr. Vincent Tam. The dedication and passion he has for research have been an inspiration for me, which keeps me always excited and enthusiastic toward my research, even during tough times in the Ph.D. pursuit. His continuous support, guidance, and immense knowledge have been my primary resource to improvise my approach to research and complete this dissertation. His guidance on both research as well as on my career have been priceless and will be the most important treasure of my future career.

I would also like to thank my committee members, Dr. Adriana E. Rosato, Dr. Diana S-L Chow, Dr. Song Gao, and Dr. Truc T. Tran for their contributions of time and ideas. Their insightful comments and discussions have improved my research from various perspectives. I would especially like to thank Dr. Tran, who shared her experience in molecular microbiology with me, and gave me access to laboratory and research facilities. Without Dr. Tran's support, it would not be possible for me to complete clonal relatedness studies within such a short time period.

The members of the PPS group have contributed immensely to my personal and professional time at UH. I am continually amazed by the caliber of faculty, staff, students, and postdocs PPS attracts, and humbled by their collective output. The group has been a source of friendships as well as good advice and collaboration.

During the last few years I have developed career-defining skills and experienced tremendous individual growth, and none of this would have been possible without the support from the group. I am especially grateful to all my present and past lab mates who have helped me in the project.

Lastly, I would like to thank my family for all their support and encouragement. I would not have made it this far without them. These past several years have not been an easy ride. I truly thank their unconditional love during my good and bad times.

ABSTRACT

Multi-drug resistant (MDR) *Acinetobacter baumannii* is increasingly more prevalent in nosocomial infections. Although *in vitro* susceptibility of *A. baumannii* to minocycline is promising, the *in vivo* efficacy of minocycline has not been well established. Moreover, the shortage of new effective antibiotics against MDR *A. baumannii* has created a need for maximizing the usage of currently available antibiotics. Therefore, we proposed to improve the therapeutic outcomes of minocycline for infections caused by *A. baumannii*. Our working hypothesis was that therapeutic outcomes could be improved by maximizing minocycline efficacy and suppressing the development of resistance in *A. baumannii*.

We intended to achieve this proposed goal by: 1) deriving PK parameters for minocycline using a murine infection model; 2) determine the exposure-response relationship of minocycline; 3) suppressing the development of minocycline resistance. Our findings will fill the gaps in knowledge needed to optimize the use of minocycline and support its role as a first-line agent in the treatment of *A. baumannii* infections. Moreover, it is anticipated that our strategies for optimizing treatment with minocycline may be applicable to other tetracyclines, thereby expanding the viable options for MDR *A. baumannii* infections.

TABLE OF CONTENTS

LIST OF FIGURES

LIST OF TABLES

CHAPTER 1: INTRODUCTION

1.1 Background

Various antibiotics have been developed since penicillin was first used in humans in 1940s. However, antimicrobial resistance has made these antibiotics less effective. As a result, there is a shortage of effective antibiotics for the treatment of life-threatening bacterial infections (1). According to the Centers for Disease Control and Prevention (CDC), at least 2 million people were infected with resistant bacteria every year in the United States, and more than 23,000 of them died (2). The spread of antimicrobial resistance also increased the economic burden of the health care system markedly. In the United States, around $55 billion were cost by antimicrobial resistance each year (3).

Acinetobacter is one of the most problematic genus among all the pathogens. Infections associated with these bacteria were classified at a “serious concern level”, in a report by the Centers for Disease Control and Prevention (CDC). About 7% of healthcare-associated infections among the critically ill patients on mechanical ventilators were caused by *Acinetobacter*, and 63% of *Acinetobacter* are multi-drug resistant (MDR) (4). As a typical representative of this genus, *Acinetobacter baumannii* is the most problematic species, because it exhibits an outstanding ability to acquire and accumulate multi-drug resistance (5, 6). *A. baumannii* is an opportunistic pathogen, which mostly affects patients with

compromised immune function. It is commonly implicated in infections of the respiratory tract, bloodstream, urinary tract and skin. In recent years, the prevalence of MDR *A. baumannii* isolates has been increasing (7). Many commonly used antimicrobial agents are ineffective, and increased mortality was reported in patients infected with MDR *A. baumannii* (8, 9). In addition, we are facing a significant shortage of effective antibiotic agents against infections caused by MDR *A. baumannii.* Thus, improving the efficacy of the currently available antibiotics is the need of the hour.

In 2013, Denys et al. collected the susceptibility data of Gram-negative bacteria from the U.S. between 2005 and 2011. In that study (n=883), the susceptibility rate of MDR *Acinetobacter* isolates to minocycline was 72.1 %, whereas most of the other drugs examined were found to be resistant (10). The i*n vitro* susceptibility results of minocycline for *A. baumannii* are promising. However, the *in vivo* efficacy was not well established yet, and the currently using dosing regimen of minocycline may not be optimal. It is well accepted that antimicrobial resistance crisis was mainly caused by misuse of antibiotics, including overuse and inappropriate prescribing (1, 11). Improved understanding of the minocycline pharmacokinetics and pharmacodynamics is urgently needed. The rationale of dosing regimen design could help improving the therapeutic outcomes of infections caused by MDR *A. baumannii*.

On the other hand, the understanding of resistance development could help us suppress it. There are various known mechanisms that are responsible for decreased susceptibility of *A. baumannii* to antibiotics. The major reported resistance mechanisms of *A. baumannii* against tetracyclines include up-regulation of efflux pump(s) and ribosomal protection (12). Tetracycline-specific efflux pumps are encoded by the *tetA* and *tetB* determinants, which could reduce intracellular concentration of tetracyclines. Ribosomal protection is regulated by *tetM,* which decreases the affinity of ribosomes to drug molecules (13, 14). In addition, multidrug efflux pumps, *adeABC* and *adeIJK*, also play an important role in tetracyclines resistance (15, 16). This type of efflux pumps could cause cross-resistance among multiple classes of antibiotics. Detoxification by enzyme and reduced uptake have been reported as tetracycline resistance mechanisms in *Escherichia coli,* other than *A. baumannii* (14). Among all the mechanisms, the most likely one(s) that emerge(s) *in vivo* during minocycline treatment is unclear.

In 2011, the study reported by Hornsey, M. and colleagues compared two *A. baumannii* isolates from a patient, by whole genome sequencing. The isolates were collected from a patient before and after receiving tigecycline. However, the author could not determine whether the change in genome was caused by the drug exposure, or the patient initially had a mixed infection (17). In contrast, the conditions of animal studies could be well controlled. Therefore, in terms of the

clonal relationship with the parent isolate, mutant derived from animal model is superior for studying resistance development.

1.2 Overview

The overall objective of the proposed research is to improve therapeutic outcomes of minocycline against *A. baumannii* infections. To achieve this objective, we plan to study various factors that affect minocycline therapeutic outcomes, and which could guide treatment strategies. The project is separated into three specific aims as shown below. Briefly, Aim 1 will be focused on the pharmacokinetics of minocycline. In Aim 2, we will establish an exposure-response relationship and strive to improve minocycline *in vivo* efficacy. Finally, Aim 3 is to study resistance development in *A. baumannii* during therapy.

1.3 Specific aims

The limited availability of new antibiotics for MDR *A. baumannii* makes it imperative for us to take a step back to assess the old antibiotics such as minocycline. Traditionally designed minocycline dosing regimen may not be optimal for MDR *A. baumannii*. Therefore, we need to optimize dosing strategies to improve therapeutic outcomes of minocycline. With the findings of the proposed project, minocycline could be re-purposed as an effective treatment against *A. baumannii* infections.

There are 3 specific aims in this project:

Aim 1: To characterize pharmacokinetics of minocycline.

Our working hypothesis for this aim is that the PK of minocycline is linear in mice, for all the dose levels we evaluate. Therefore, we can use the best-fit PK parameters to simulate the corresponding drug exposure for different dosing regimens. We will test our hypothesis by performing PK studies with different minocycline dose levels.

Aim 2: To maximize minocycline *in vivo* efficacy.

Our working hypothesis for this aim is that minocycline exposure is correlated to the reduction of *in vivo* bacterial burden. Therefore, efficacy could be improved by optimizing the dosing regimen. We will test our hypothesis by establishing the exposure-response relationship of minocycline.

Aim 3: To study *in vivo* resistance development in *A. baumannii.*

Our working hypothesis for this aim is that development of minocycline resistance in *A. baumannii* can be suppressed by optimizing factors linked to resistance development. Therefore, understanding the mechanism(s) of resistance development could help improve therapeutic outcomes. We will test our hypothesis by studying *A. baumannii* resistance development in an animal infection model.

CHAPTER 2: LITERATURE REVIEW

2.1 Minocycline

Minocycline, a semi-synthetic derivative of tetracycline, was approved by FDA in 1970. It has a broad spectrum of activity against Gram-positive and Gram-negative bacteria. By binding to the 30S ribosomal sub-unit, minocycline can inhibit protein synthesis in bacteria. Compared to other tetracyclines, it has excellent penetration into tissues and a long elimination half-life (18, 19). Both of these are favorable pharmacokinetic properties. Conventionally, minocycline has not been used as a first-line agent in Gram-negative bacterial infections. However, the shortage of new and effective antibiotics against MDR *A. baumannii,* has motivated us to re-evaluate the utility of minocycline. Despite good *in vitro* results of minocycline against MDR *A. baumannii*, satisfactory clinical response was not consistently seen in patients treated with minocycline (20). A higher minocycline daily dose may be necessary for infections caused by MDR *A. baumannii*. Although the typical dosing regimen of minocycline is 200 mg/day, 400 mg IV q12h with an 800 mg loading dose has been used in humans, for acute spinal cord injury (21). Therefore, a higher and safe dose of minocycline in human might be feasible. However, the *in vivo* efficacy of minocycline has not been well established and the rationale of the minocycline dosing regimen design needs to be further substantiated.

Information about bio-distribution of minocycline is limited. In this study, we mainly focused on pneumonia, but data regarding pulmonary exposure of minocycline in humans is not available. Although a minocycline bio-distribution study has been performed in healthy rats by Nagpal, *et al*, infected animals have not been studied yet (22). Inflammation, which is caused by infections, might change the permeability of minocycline into lung tissues, as well as the volume of distribution. Therefore, we need to characterize pharmacokinetics of minocycline in both serum and ELF for the infected animals.

In addition, serum protein binding is critical for understanding the pharmacokinetics and pharmacodynamics of antimicrobial agents. Only the free fraction is able to penetrate into extravascular space and exert antimicrobial effects. Serum protein binding of minocycline is usually accepted as 76%, which was determined by ultrafiltration (23). However, antimicrobial agents may show non-linear protein binding due to the saturation of binding sites, and typically the percentage of free fraction increases, with increasing total concentration (24, 25). Recently, a contrary phenomenon was reported in tigecycline and eravacycline (26-28). The percentage of free fraction decreased with increasing total concentration. It was suggested that the phenomenon could be due to the chelating effect of tetracyclines to divalent metal ions (29). It is possible that other tetracyclines would also have the same property (i.e., a class effect). Therefore,

we investigated different factors that might impact the binding of minocycline to serum proteins.

2.2 Hospital-acquired pneumonia

Hospital-acquired pneumonia (HAP), or nosocomial pneumonia, refers to pneumonia occurring at least 48 hours after being admitted in the hospital (30). HAP is the second most commonly occurring nosocomial infection (after urinary tract infections) (31), and is also the most important cause of death among all the hospital-acquired infections (32). In a multistate point-prevalence survey published in 2014, HAP accounted for around 22% of all the nosocomial infections (33). Usually, HAP is considered to include ventilator-associated pneumonia (VAP) and healthcare-associated pneumonia (HCAP). VAP is defined as pneumonia occurring more than 48 to 72 hours after endotracheal intubation, while HCAP is defined as pneumonia occurring outside the hospital, but with the patients having close contact with the healthcare system (31).

HAP is mainly caused by Gram-negative bacteria, such as *Pseudomonas aeruginosa*, *Escherichia coli*, *Klebsiella pneumoniae*, and *Acinetobacter* species. In addition, methicillin-resistant *Staphylococcus aureus* (MRSA) is also an important pathogen for HAP (33). It was reported that age, male sex, structural lung disease and multi-organ system failure are factors which could increase the risk of HAP (33). About 1/3 of the HAPs occurred in intensive care unit (ICU), and 90% of them were VAP (34). The neutropenic murine pneumonia model was

used in our project, to mimic the physiological conditions of HAP patients. Details of the model have been demonstrated previously (35). Serum tumor necrosis factor α (TNF-α) and interleukin 6 (IL-6) were found to be significantly higher in infected mice compared with control group, which was similar to the physiological conditions of patients with bacterial infections (36). Furthermore, two doses of cyclophosphamide administered prior to the experiments could induce neutropenia which mimics the condition of immunocompromised patients, who are usually vulnerable to HAP.

2.3 Pharmacokinetic/ Pharmacodynamic (PK/PD) modeling of antibiotics

In 2013, about 23000 deaths were caused by drug resistant bacteria in the U.S, while the number was 25000 in Europe (37). Misuse and sub-optimal dosing of antibiotics could be important reasons for treatment failure (38). On the other hand, over-dosing drugs will increase the risk of side effects and the cost of treatment. Therefore, to optimize dosing regimens of antibiotics, we have to understand the relationship between drug exposure and bacterial response.

For antibiotics, the exposure of the drug in the human body (pharmacokinetics) and the response of bacterial pathogen to the drug (pharmacodynamics) could be linked by a PK/PD index. There are three commonly used PK/PD indices: the peak concentration and minimum inhibitory concentration ratio (C_{max}/MIC), percentage of dosing interval that drug concentration is above MIC (%T>MIC) and area under the concentration-time curve to MIC ratio (AUC/MIC). The PK/PD

index is determined by the killing property of the antibiotics: C_{max}/MIC is used when antimicrobial activity is concentration-dependent; %T>MIC is used when antimicrobial activity is time-dependent; AUC/MIC could be used when antimicrobial activity is both concentration and time dependent (38). Usually, the best PK/PD index for an antibiotic is determined by a dose fractionation study. With a fixed daily dose, the drug could be administered as a single dose or smaller doses with different dosing intervals. The most appropriate PK/PD index could be identified by comparing the correlation between PK/PD indices and the bacterial responses (39). The antimicrobial activities of tetracyclines are usually considered as both concentration and time dependent. Therefore, AUC/MIC is expected to be the most appropriate PK/PD index for minocycline.

The relationships between the best PK/PD indices and the bacterial responses could be described by an inhibitory sigmoid E_{max} model (40). With the knowledge of exposure-response relationship, the magnitudes of PK/PD indices for the required PD targets could be calculated. Clinicians are able to select the optimal dosing regimens for the patients and minimize the risk of side effects.

2.4 Resistance development

The emergence of resistance is a major problem in antimicrobial therapy. Increased mortality, cost and patients' suffering make it imperative for us to understand and suppress the development of resistance. There are three commonly accepted mechanisms responsible for bacterial adaptation to the

selective conditions. First, the adaptation is caused by altered regulatory mechanisms, rather than genetic change; second, the mutation is associated with increased copy of gene, which is called gene duplication-amplification (GDA) (increased level of enzyme or efflux pumps, etc.); third, the mutation is genetically stable, e.g., frameshift, deletion and insertion, etc. The gene regulatory response and GDA are usually common and reversible, whereas the third one is rare. Therefore, it was considered that GDA is the intermediate step of stable genetic mutation (41). Various technologies could be utilized to detect genetic mutations, including real-time quantitative PCR and next generation genome sequencing, etc.

During exposure to antimicrobial treatment, there are two ways for bacteria to gain genetic resistance: acquired and *de novo*. In acquired resistance, mobile genetic elements are obtained from other bacteria, whereas *de novo* is developed in a step-wise manner through the mechanisms described above (42). In this project, we focused on suppressing the *de novo* pathway in *A. baumannii*. The minimum inhibitory concentration (MIC) of antibiotic may inhibit the visible growth of micro-organisms, but may not kill resistant sub-populations. To suppress the development of resistance, the mutant prevention concentration (MPC) is required. Thus, the MPC is the MIC of the most resistant subpopulation. According to the mutant selection window hypothesis, the selection window (concentration range between MPC and MIC_{99}, which is drug concentration that

inhibits 99% of the subpopulations) is problematic, in terms of selective amplification of resistant sub-populations (43). Traditional dosing strategies tend to selectively amplify the resistant subpopulations during treatment, since MICs of parent isolates are usually used to design dosing regimens. Therefore, maintaining the drug concentration above the selection window is the best practice for avoiding resistance development (44). In the drug development stage, candidates with a narrow selection window are more promising than those with simply low MICs. The findings of the current project will help to optimize regimens to suppress resistance development in *A. baumannii*.

CHAPTER 3: GENERAL METHODS

3.1 *In vitro* microbiology studies

3.1.1 Quantitative culture

Quantitative culture is a technique for quantifying bacteria in the sample. Briefly, samples were serially diluted with sterile saline (transferring 100 µL sample into 900 µL saline). An aliquot of sample (200 µL) was dropped onto the Mueller-Hinton agar (MHA) plate, and spread using the wet sterile cotton swab. The plates were incubated at 37°C overnight. A valid colony number (n) should be between 20 and 200. The bacterial burden was calculated as $Log_{10}(n*5)$ + dilution factor, and the unit of bacterial burden was log_{10} CFU/mL.

3.1.2 Minimum inhibitory concentrations

The minimum inhibitory concentrations (MICs) were defined as the lowest concentrations of chemicals that inhibit the visible growth of micro-organisms. The values indicate susceptibility of micro-organisms to the chemicals. MIC could be determined in liquid growth medium (broth) or on the surface of solid growth medium (agar). In the current project, both broth dilution method and ETEST approach were used to determine MICs of various antibiotics against the *A. baumannii* isolates.

3.1.2.1 Broth dilution method

The protocol of broth dilution method followed the guidance of the Clinical and Laboratory Standards Institute (CLSI) (45). A concentration range which includes the anticipated MIC value was chosen for the antibiotic. The antibiotic was serially diluted by cation-adjusted Mueller-Hinton broth (Ca-MHB) into twice as much of the desired concentrations. An aliquot of 250 µL antibiotics was mixed with equal volume of bacterial suspension (10^6 CFU/mL of bacteria in Ca-MHB). Negative control was filled with 500 µL of Ca-MHB, while positive control was a mixture of 250 µL Ca-MHB and an equal volume of the bacterial suspension. Tubes were incubated at 37°C for 16 - 20 hours, and vortexed again. The MIC values were read at 24h of incubation. MIC of the antibiotic was the lowest concentration that the corresponding tube was clear.

3.1.2.2 ETEST

In ETEST method, the antibiotics were preloaded on a plastic strip, and the MICs were determined by the bacterial inhibition zone. Briefly, the concentration of bacterial cell suspension in Ca-MHB was adjusted to 0.15-0.25 absorbance at 590nm wavelength. The suspension was spread on the MHA plates by a sterile cotton swab within 20 minutes. The excess moisture could be absorbed by the agar completely, after approximately 15-20min. ETEST strips were applied to the surface of inoculated agar with forceps. The air pockets under the strip could be removed by pressing gently on the strip without moving it. Agar plates were

incubated at 37 °C for 16-20 hours, and the lowest concentration of the inhibition zone was the corresponding MIC.

3.2 Neutropenic murine pneumonia model

A neutropenic murine pneumonia model was used in this project. The experimental setup was as previously described (35, 46). Female Swiss Webster mice weighing between 20 and 25 g (Harlan, Indianapolis, IN) were rendered neutropenic by two doses of intraperitoneal cyclophosphamide, prior to the experiment (150 mg/kg in day -4 and 100 mg/kg in day -1). Neutropenia could minimize the impacts of innate immune function and therefore reduce the inter-subject variability of the animals.

The animals were anesthetized by one dose of intraperitoneal 1.25% Avertin (2, 2, 2-Tribromoethanol) (approximate 0.3 mL). Avertin was prepared by mixing 125 mg 2,2,2-tribromoethanol and 0.25 mL tert-amyl alcohol (Sigma-Aldrich) with 10 mL injection water. An overnight culture of bacteria was inoculated in fresh broth, and grown to log phase. Then the bacterial suspension was concentrated to the desired burden, on the basis of absorbance at 630 nm. The anesthetized mice were inoculated with approximately 10^7 - 10^8 colony forming unit (CFU) of *A. baumannii* under laryngoscopic guidance. The protocol was approved by Institutional Animal Care and Use Committee of the University of Houston. The immune response in mice after infection has been studied previously in our lab. Serum tumor necrosis factor α (TNF-α) and interleukin 6 (IL-6) were found to be

significantly higher in the infected mice, compared with the control group (36). The results were consistent with the pathophysiology of patients with severe pneumonia (47).

3.3 LC-MS/MS assay method development

The liquid chromatography-tandem mass spectrometry (LC-MS/MS) was used to determine drug concentrations in serum and epithelial lining fluid (ELF) samples. The LC-MS/MS system consists of a Waters Acquity^{TM} UPLC with Waters BEH C_{18} column (1.7μm 2.1x50mm) and API5500 Qtrap triple quadrupole mass spectrometer (Applied Biosystem/MDS SCIEX, Foster City, CA, USA) equipped with Turbo-Ion-Spray ^{TM} source. The mobile phase A and B were 0.1% formic acid in distilled water and acetonitrile, respectively.

3.3.1 Chromatographic and mass spectrometric conditions

In the Ultra Performance Liquid Chromatography (UPLC) system, analytes were separated by gradient elution, which was: 0-0.5min: 98% A; 0.5-0.7min: 98-84% A; 0.7-1.2 min: 84-76% A; 1.2-1.7min: 76-70% A; 1.7-2.1min: 70-50% A; 2.1-2.5 min: 50-5% A; 2.5-3.0min: 5% A; 3.0-3.2min: 5-98% A; 3.2-5min: 98% A. The flow rate was set at 0.35 ml/min, and the temperature of the column was 45°C. The temperature of the sample chamber was maintained at 15°C. For the mass spectrum, the curtain gas, ionspray voltage, temperature, ion source gas 1 and gas 2 were 20, 5000 V, 500°C, 35 and 40, respectively.

3.3.2 Assay method validation

For all the tested compounds, the methods have been validated at three different concentration levels (L: low, M: medium, H: high). LLOQ (Lowest Limit of Quantification) was defined as the concentration of drug peak with 10 times height of baseline, while HLOQ (Highest Limit of Quantification) was the highest concentration tested in the validation. For different compounds, the sample preparation procedures will be described in Chapter 4.

3.3.2.1 Standards and quality controls

Stock solutions of antibiotics (8192 mg/L) were prepared by dissolving drugs in water separately, and stored at -80°C. The stock solutions were thawed for preparing standard solutions prior to experiments, and serially diluted with distilled water or 0.5% (V/V) methyl-sulfoxide (DMSO). Quality control samples (QC) were made by diluting stock solution into different concentrations with serum or ELF, and stocked in -80℃.

3.3.2.2 Accuracy and precision

Accuracy and intra-day precision were determined by analyzing 6 QC samples for each concentration level within 1 day. The inter-day precision was assessed by repeating the same experiment twice on different days. Therefore, there were 6 samples for intra-day precision and 18 samples for inter-day precision, at each concentration level. Meanwhile, a standard curve generated by serially diluted

standards was prepared every day. According to the standard curve, concentration of each sample was determined. Accuracy was calculated as the average concentrations of QC divided by the nominal values, while precision was calculated as the standard deviation of the QC concentrations divided by their mean values (coefficient of variation).

3.3.2.3 Recovery and matrix effects

The recovery and matrix effects of 3 concentration levels were evaluated (L, M, H). Three different sets of samples were analyzed for determining recovery and matrix effects, and all the samples were triplicated. Set A was prepared in the same method as QC. Set B was the neat solution of analytes (dissolved in 10% acetonitrile for levofloxacin or in 50% methanol for minocycline and doxycycline). Set C was prepared by reconstituting blank matrix residual with set B. The peak area of analytes was used for calculation. Recovery was the ratio between set A and set C values, and matrix effects was the ratio between set C and set B values.

3.3.2.4 Data analysis

The results were analyzed in Multiquant 2.0.2. The $1/X^2$ weighted linear regression was used for the standard curves. The acceptable accuracy range of each concentration level is 85-115%, and the precision must be within 15%. The

extent of recovery should be close to 100%, while matrix effects should be close to 0. Both of them have to be consistent across all concentration levels.

CHAPTER 4: PHARMACOKINETICS OF MINOCYCLINE

To translate our findings clinically, we need to explore the pharmacokinetics of minocycline in the neutropenic murine pneumonia model. The results of our studies could be correlated to patients in terms of the relevant drug exposure (AUC, concentration, etc.). In this chapter, we developed and validated a LC-MS/MS assay method for minocycline in mouse serum and ELF. The assay methods of doxycycline and levofloxacin in mouse serum were also validated. The serum protein binding of minocycline was investigated by an *in vitro* microdialysis system. Finally, a modified 2-compartment PK model was used to fit the minocycline serum and ELF concentration data.

4.1 Materials and methods

4.1.1 Materials

Liquid chromatography-mass spectrometry (LC-MS)-grade water, methanol and acetonitrile were purchased from EMD Millipore Corporation (Billerica, MA). Methyl-sulfoxide (DMSO) was obtained from EM SCIENCE (Gibbstown, NJ). LC-MS-grade formic acid, minocycline hydrochloride, doxycycline hyclat, HEPES, dipotassium phosphate (K_2HPO_4) and monopotassium phosphate (KH_2PO_4) were purchased from Sigma-Aldrich (St. Louis, MO). Mouse and human sera were obtained from Equitech-Bio, Inc (Kerrville, TX). Mueller Hinton II Broth (cation-adjusted) was manufactured by BD Diagnostic Systems Europe. The

urea assay kit was from BioAssay Systems (Hayward, CA). CMA 12 Elite Microdialysis Probe was a product of CMA Microdialysis (Reference number 8010434; Stockholm, Sweden). The semi permeable membrane (20,000 Da cut-off) was made of polyarylethersulfone (PAES).

4.1.2 LC-MS/MS assay

4.1.2.1 Minocycline and doxycycline

The chromatographic conditions have been described in section 3.3.1. The multiple-reaction monitoring (MRM) scan type in positive mode was used for mass spectrum. The transitions were m/z 458.3 to 441.2 and m/z 445.2 to 154.2 for minocycline and doxycycline, respectively. The declustering potential (DP), collision energy (CE) and collision cell exit potential (CXP) of minocycline were 55, 25 and 20; while the values of doxycycline were 50, 23 and 20, respectively.

The sample preparation procedures were similar for these 2 drugs, and they were used as internal standard for each other. For standards, 10 µL of blank serum or ELF was mixed with 10 µL of standard solutions (0.5% DMSO, V/V) and 30 µL of internal standard solution (10 µg/ml in water). For serum or ELF samples, 10 µL of sample was mixed with 10 µL of 0.5% DMSO (V/V) and 30 µL of internal standard solution (10 µg/ml in water). Each tube was added 170 µL of acetonitrile (containing 0.03% formic acid, V/V). After vortexing for 30 seconds, the samples were centrifuged for 15 minutes at 18000x g. An aliquot of 40 µL

supernatants were transferred to a new tube, and evaporated under a stream of ambient air. After being reconstituted with 1 mL of 50% methanol, 5 µL of the samples were injected into the UPLC system. The assay methods were validated as described in section 3.3.2.

4.1.2.2 Levofloxacin

The chromatographic conditions for levofloxacin were similar to that for minocycline and doxycycline. The multiple-reaction monitoring (MRM) scan type in positive mode was used. The transitions were m/z 362.1 to 318.1 and m/z 332.1 to 268.3 for levofloxacin and ciprofloxacin (internal standard), respectively. The DP, CE and CXP of levofloxacin were 65, 25 and 20; while the values of ciprofloxacin were 40, 30 and 11, respectively.

For standards, 10 µL of blank serum was mixed with 10 µL of standard solutions and 20 µL of internal standard (ciprofloxacin in 1% ammonium hydroxide, 8 mg/L). For samples, 10 µL of serum samples were mixed with 10 µL of distilled water and 20 µL of internal standard (ciprofloxacin in 1% ammonium hydroxide, 8 mg/L). Each tube was added 170 µL of acetonitrile. After vortexing for 15 seconds, the samples were centrifuged for 15 minutes at 18000X g. An aliquot of 20 µL supernatants were transferred to a new tube, and mixed with 220 µL of distilled water. The samples were ready for analysis, and the injection volume was 3 µL. The assay methods were validated as described in section 3.3.2.

4.1.3 Serum protein binding

4.1.3.1 Microdialysis

Serum protein bindings of minocycline, doxycycline and levofloxacin were determined by *in vitro* microdialysis as described previously (26, 48). Briefly, a probe was inserted into a reservoir tube (containing serum spiked with an antimicrobial agent, incubated at 37°C). The perfusion medium was perfused through probe at the flow rate of 1.5 µL/min. The system was equilibrated for 30 minutes, and then dialysates were collected between 30-40 and 40-50 minutes. Concurrent samples from reservoir tube were also collected at 30, 40 and 50 minutes. Recovery of the microdialysis system was determined similarly and separately for each experiment; the reservoir tube was filled with a perfusion medium instead of serum. To minimize the non-specific binding of drugs to the tubing and membrane, the system was pre-conditioned by the same setup for 50 minutes. The experiments were performed at least twice on different days and the free fraction was calculated by the average of the results. Schematic microdialysis setup was shown in Figure 1, and the serum protein bindings were calculated by the equations below.

Figure 1: Schematic microdialysis setup for protein binding determination

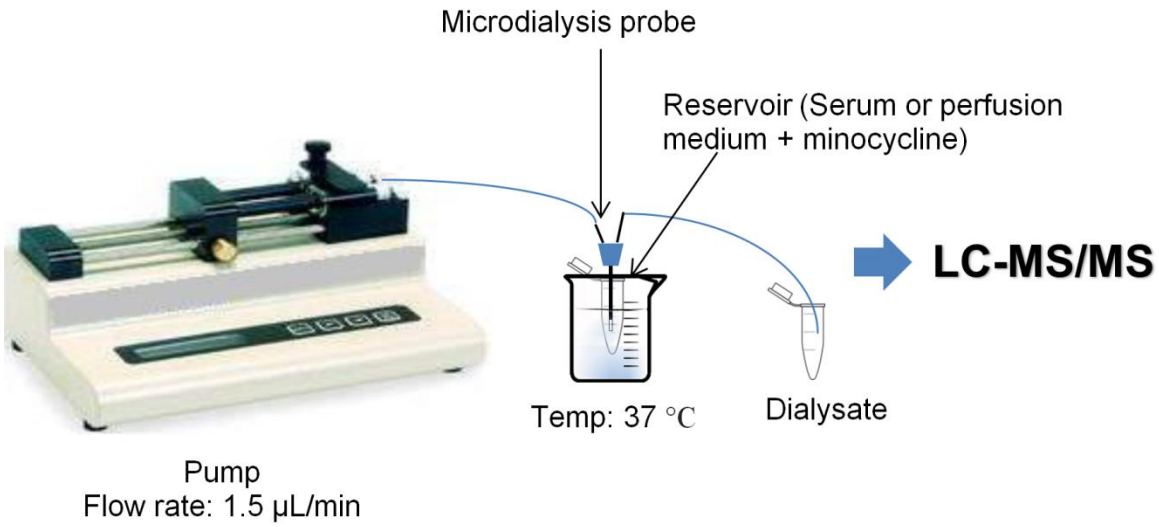

$$\text{Recovery} = \frac{2 \times C_{d,recovery}(T1,T2)}{C_{r,recovery}(T1)+C_{r,recovery}(T2)}$$

$$\text{Free fraction} = \frac{2 \times C_{d}(T1,T2)}{C_{r}(T1)+C_{r}(T2)} \times \frac{1}{\text{Recovery}}$$

Where $\mathbf{C_d\,(T1, T2)}$: Dialysate concentration collected between time 1 and time 2;

$\mathbf{C_r}$: Concentration of sample taken from reservoir tube

4.1.3.2 Time-kill

Time-kill study was used as functional verification of minocycline serum protein binding. Studies performed previously in our lab suggested that the growth profile of *A. baumannii* in serum was similar as that in half-strength cation-adjusted Mueller-Hinton broth (0.5X Ca-MHB) (49). Briefly, the *A. baumannii* isolate was inoculated into 5mL sterile mouse serum or 0.5X Ca-MHB, and the inoculum was approximately 5×10^5 CFU/mL. The bacteria were incubated in a shaker water bath at 37°C. Serial samples were collected at different time points over 6h. Samples were centrifuged at 10000X g and 4°C for 15min, the supernatants were subsequently replaced by same volume of sterile saline. Finally, bacteria were quantified by quantitative culture as described in section 3.1.1.

4.1.4 Minocycline *in vivo* exposure

The single-dose pharmacokinetics of minocycline in mouse serum and ELF were characterized. The neutropenic murine pneumonia model was described in section 3.2. Minocycline was administered intraperitoneally in 67 animals 2h after infection. Serum or bronchoalveolar lavage (BAL) samples were collected serially over time (n≥3 for each time point). Blood samples were collected by cardiac puncture. BAL samples were recovered through the trachea after 1 mL of saline was injected into the lungs. Minocycline concentrations were determined by the LC-MS/MS method as detailed in 4.1.2.1. The minocycline concentrations in ELF were calculated by correcting minocycline concentrations in BAL with urea

concentrations as described previously (50). The serum and ELF concentration-time profiles were co-modelled by a modified two compartmental model in ADAPT 5 (51) (as shown in Figure 2). Three regimens were initially evaluated: 25 mg/kg, 50 mg/kg and 100 mg/kg. Based on the preliminary results, a humanized regimen mimicking the human serum concentration-time profile of minocycline (when a clinical dose of 200 mg is given intravenously to humans) was validated. The area under the curve (AUC) of the serum and ELF concentration-time profiles were derived by integrating the best-fit instantaneous concentrations with respect to time. Pulmonary penetration ratio of minocycline was estimated by the AUC ratio of ELF to serum.

Figure 2: Structure of the pharmacokinetic model

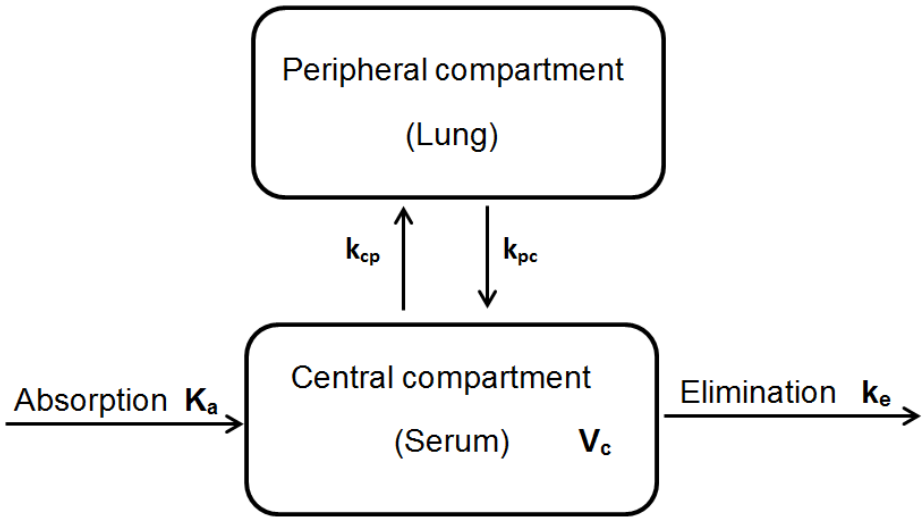

Differential equations:

$$dA_{serum} / dt = k_a \times A_{depot} + k_{pc} \times A_{ELF} / P - (k_{cp} + k_e) \times A_{serum}$$

$$dA_{ELF} / dt = k_{cp} \times A_{serum} - k_{pc} \times A_{ELF} / P$$

$$dA_{depot} / dt = - k_a \times A_{depot}$$

A_{depot}: Amount of minocycline in depot created by IP injection

A_{ELF} and A_{serum}: Amount of minocycline in ELF and serum;

k_{cp}, k_{pc}: Inter-compartmental transfer rate constants;

k_a, k_e: Absorption and elimination rate constants;

P: Minocycline penetration ratio between lung ELF and serum.

4.2 Results

4.2.1 LC-MS/MS assay

4.2.1.1 Minocycline and doxycycline

The retention times of minocycline and doxycycline were 2.5 and 3.1 minutes, respectively. The chromatogram was shown in Figure 3. The linear range of minocycline and doxycycline were 0.0625-128 mg/L and 0.125-64 mg/L, respectively (as shown in Figure 4). The results of LC-MS/MS assay validation were shown in Table 1.

Figure 3: Chromatogram of minocycline and doxycycline

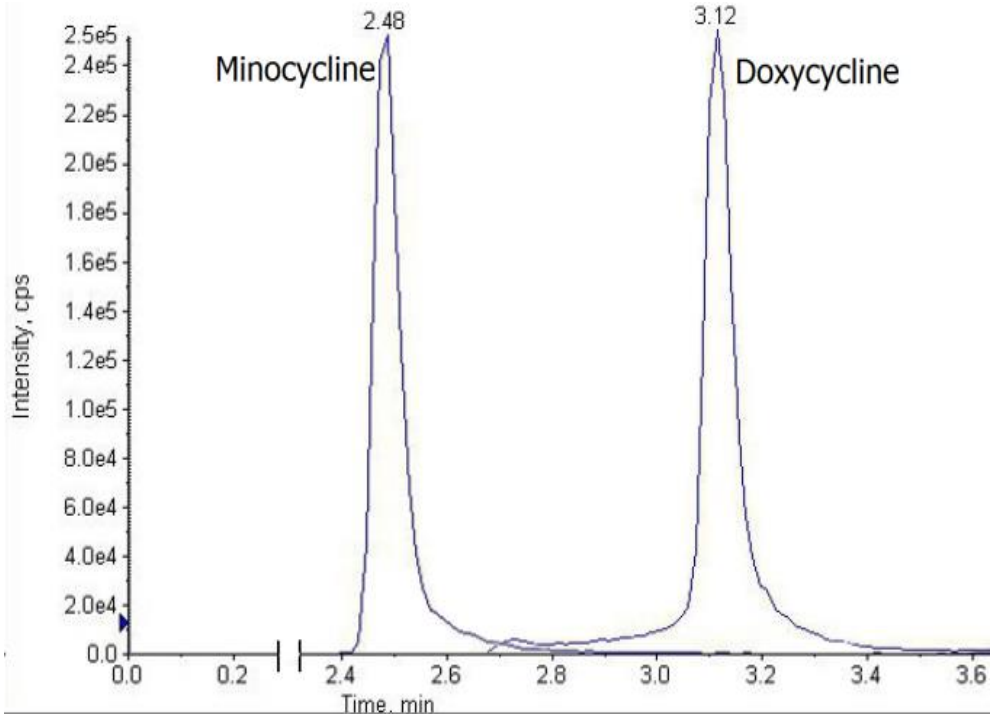

Figure 4: Calibration curve of minocycline and doxycycline

A. Minocycline

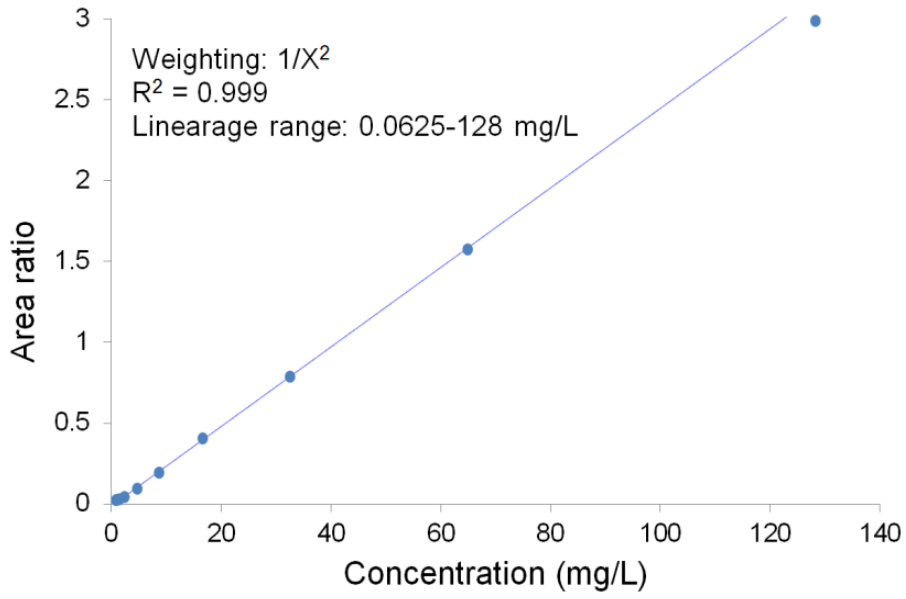

B. Doxycycline

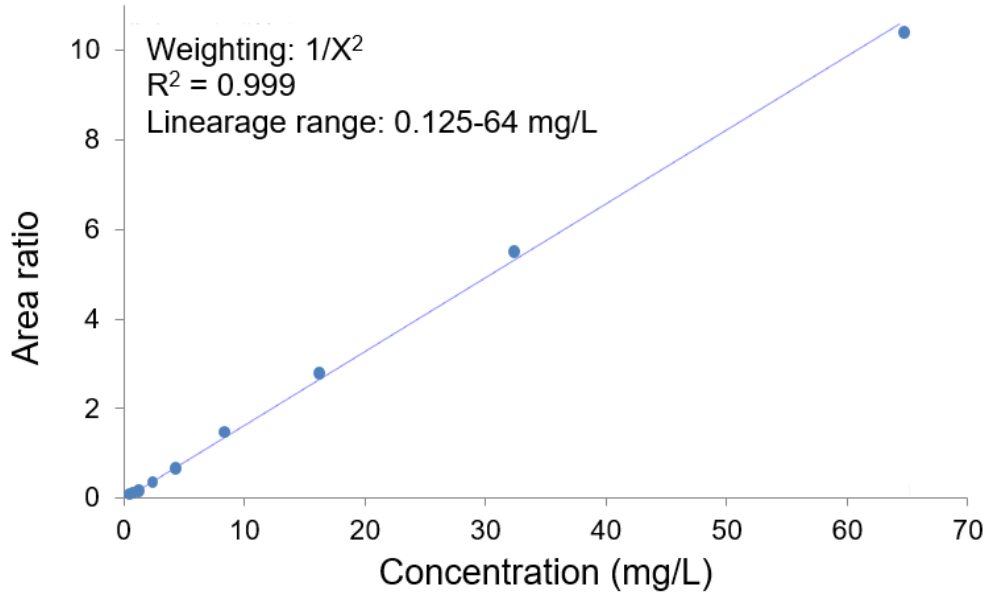

Table 1: Validation of minocycline and doxycycline LC-MS/MS assay

A. Minocycline

Matrix			L (0.5mg/L)	M (8mg/L)	H (128mg/L)
Mouse serum	Intra-day (n=6)	Accuracy	101.2%	101.1%	99.6%
		Precision	2.5%	2.2%	2.3%
	Inter-day (n=18)	Accuracy	100.5%	101.6%	96.5%
		Precision	3.4%	3.4%	3.6%
	Recovery (n=3)		102.4%	98.8%	101.4%
	Matrix effects (n=3)		89.1%	100.2%	103.1%
Mouse ELF	Intra-day accuracy (n=6)		102.4%	89.7%	96.9%
	Matrix effects (n=3)		97.5%	89.0%	88.1%

B. Doxycycline

Matrix			L (0.25mg/L)	M (4mg/L)	H (64mg/L)
Mouse serum	Intra-day (n=6)	Accuracy	103.5%	94.8%	116.5%
		Precision	9.0%	7.0%	6.7%
	Recovery (n=3)		132.0%	95.1%	104.5%
	Matrix effects (n=3)		97.8%	104.2%	96.9%

4.2.1.2 Levofloxacin

The retention times of levofloxacin and ciprofloxacin were both 2.3 minutes. The chromatogram was shown in Figure 5. The linear range of levofloxacin is 0.25-64mg/L (as shown in Figure 6). The results of LC-MS/MS assay validation were shown in Table 2.

Figure 5: Chromatogram of levofloxacin and ciprofloxacin

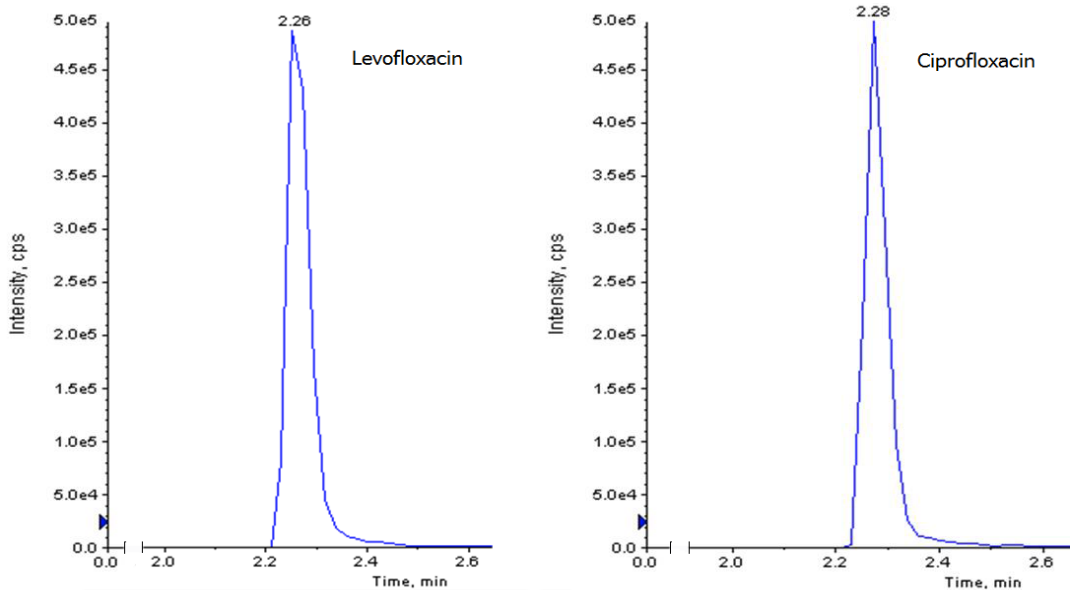

Figure 6: Calibration curve of levofloxacin

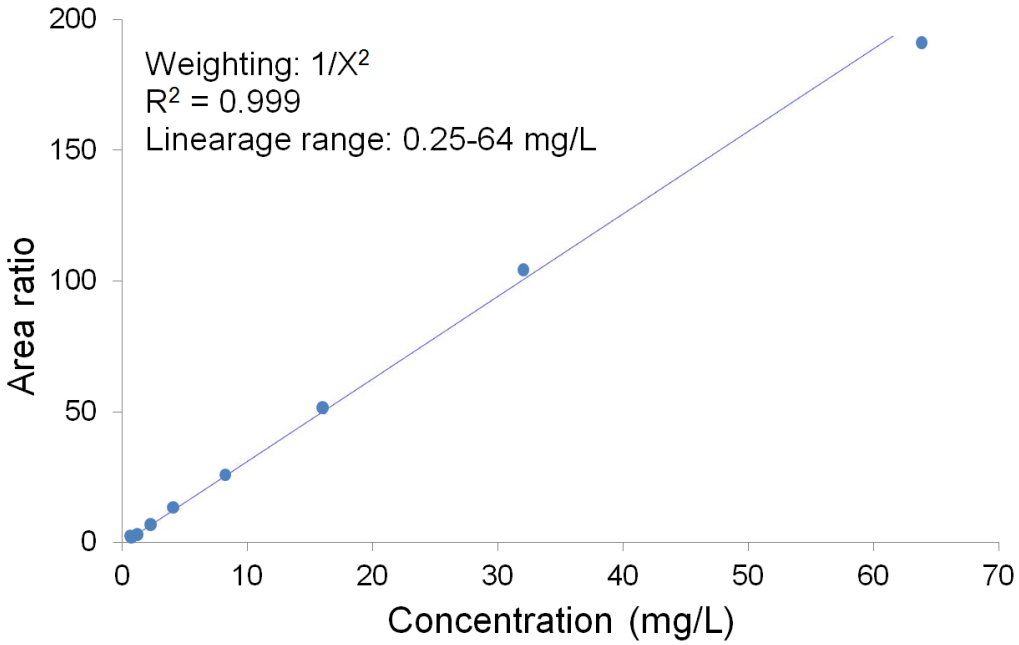

Table 2: Validation of levofloxacin LC-MS/MS assay

Matrix			L (2mg/L)	M (16mg/L)	H (64mg/L)
Human serum	Intra-day (n=6)	Accuracy	100.5%	98.7%	94.9%
		Precision	5.7%	4.5%	6.7%
	Inter-day precision (n=18)		10.0%	11.3%	8.6%
	Recovery (n=3)		105.3%	97.0%	112.5%
	Matrix effects (n=3)		85.2%	91.2%	81.2%

4.2.2 Serum protein binding

4.2.2.1 Microdialysis

The protein binding of minocycline in mouse serum was studied at 4 concentrations (0.5, 5, 15 and 50 mg/L), and 4 perfusion media [saline (sterile 0.9% (W/V) sodium chloride solution), 0.1M HEPES buffer (pH=7.4, adjusted by sodium hydroxide), 0.1M and 1M PBS (pH=7.4)] were used. Both sterile and un-processed mouse sera were used in the study, and no difference was observed. Free fractions of minocycline were shown in Figure 7. For all the perfusion media examined, the values decreased with the increase of total minocycline concentrations. Of note, the binding values could also vary among various perfusion media using the same total minocycline concentration. Compared to the buffer groups, the saline group had considerably lower free fraction values.

Similar experiments were performed using human serum and a consistent trend was observed to that in mouse serum (Figure 8). Finally, protein bindings of doxycycline and levofloxacin in mouse serum were also determined at 3 concentrations (0.5, 5 and 50 mg/L), using saline as the perfusion medium. The free fractions of doxycycline and levofloxacin in mouse serum were shown in Figure 9. Doxycycline had a similar trend of concentration-dependent protein binding, but the free fractions were slightly higher than that of minocycline. On the contrary, the protein binding values for levofloxacin were similar, and consistent with previously reported values (24 to 38%) (52).

Figure 7: Free fraction of minocycline in mouse serum

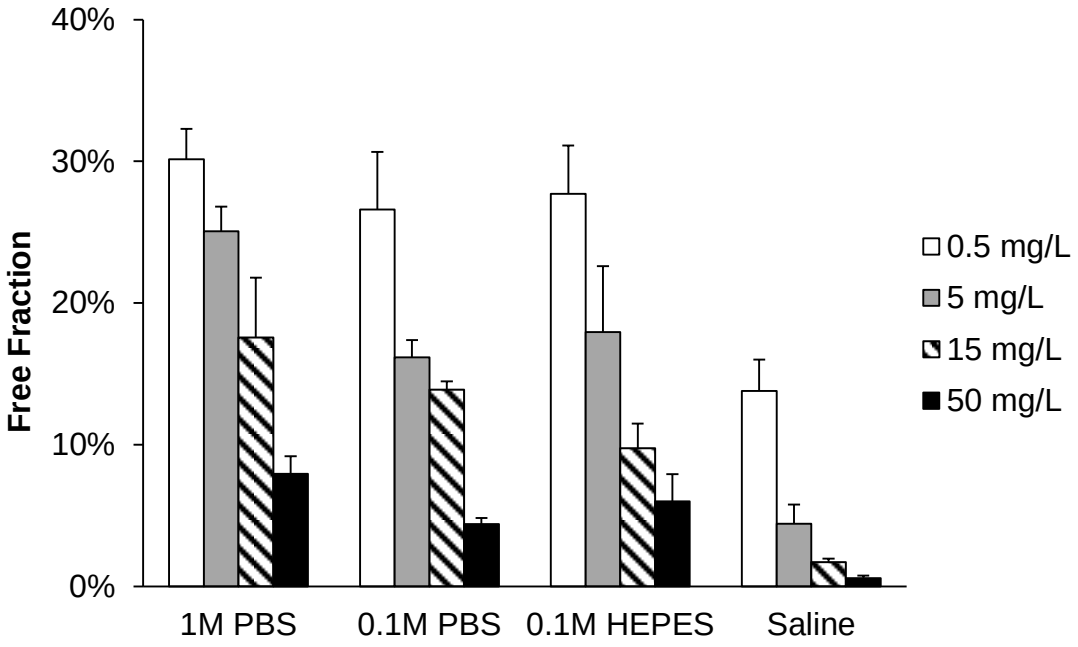

Note: Data shown as mean ± SD. Different media were used for perfusion.

Figure 8: Free fraction of minocycline in mouse and human sera

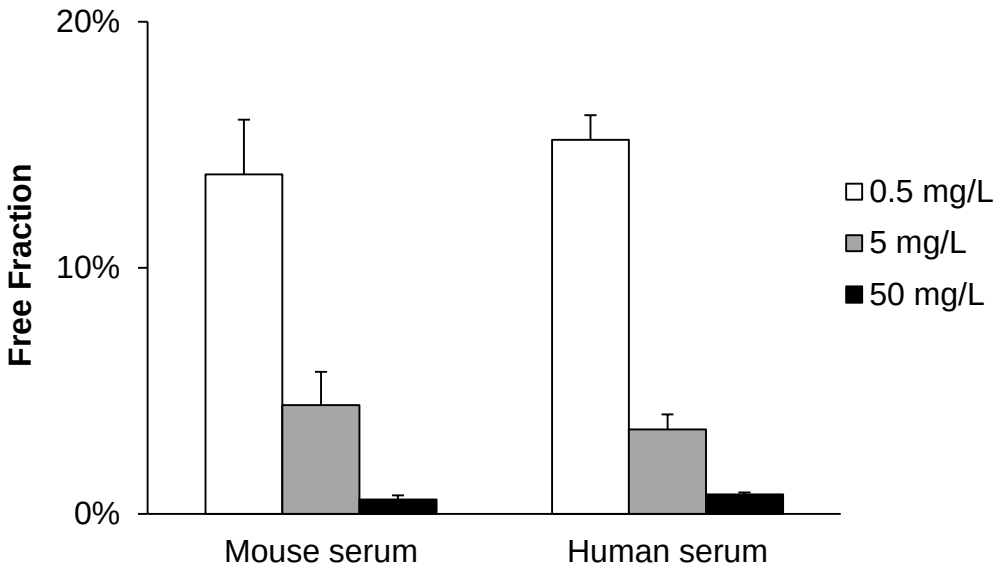

Figure 9: Free fraction of minocycline, doxycycline and levofloxacin in mouse serum

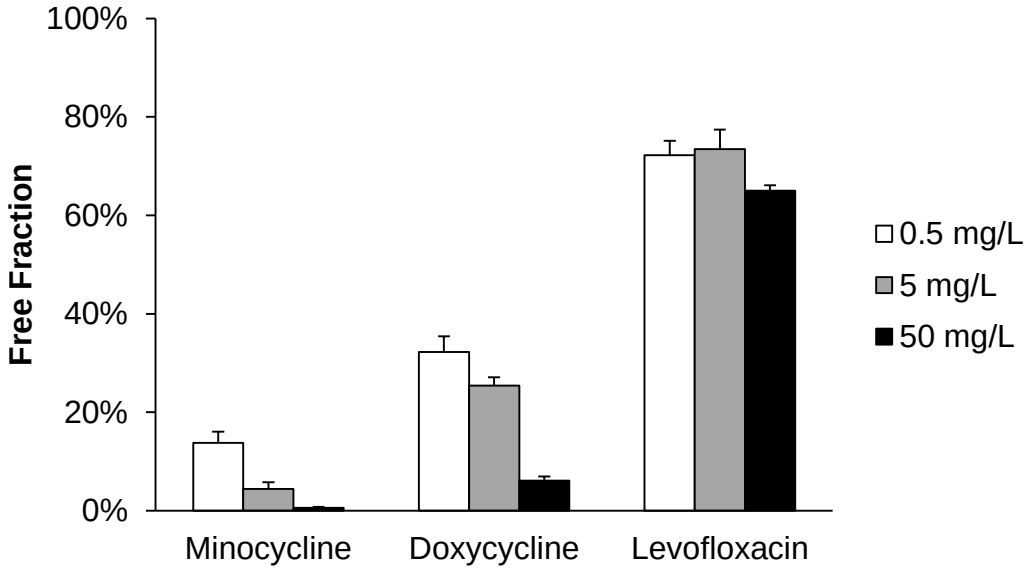

Note: Data shown as mean ± SD. Saline was used as the perfusion medium.

4.2.2.2 Time-kill

The growth profile of AB BAA 747 in mouse serum was comparable to that in half strength Ca-MHB (as shown in Figure 10). The profile of 2 mg/L minocycline in serum was comparable to that of 0.05 mg/L minocycline in 0.5X Ca-MHB. However, when minocycline concentration in 0.5X Ca-MHB increased to 0.1 mg/L, the corresponding profile in serum required 50 mg/L minocycline (as shown in Figure 11).

Figure 10: Time-kill results of placebo in serum or 0.5X Ca-MHB

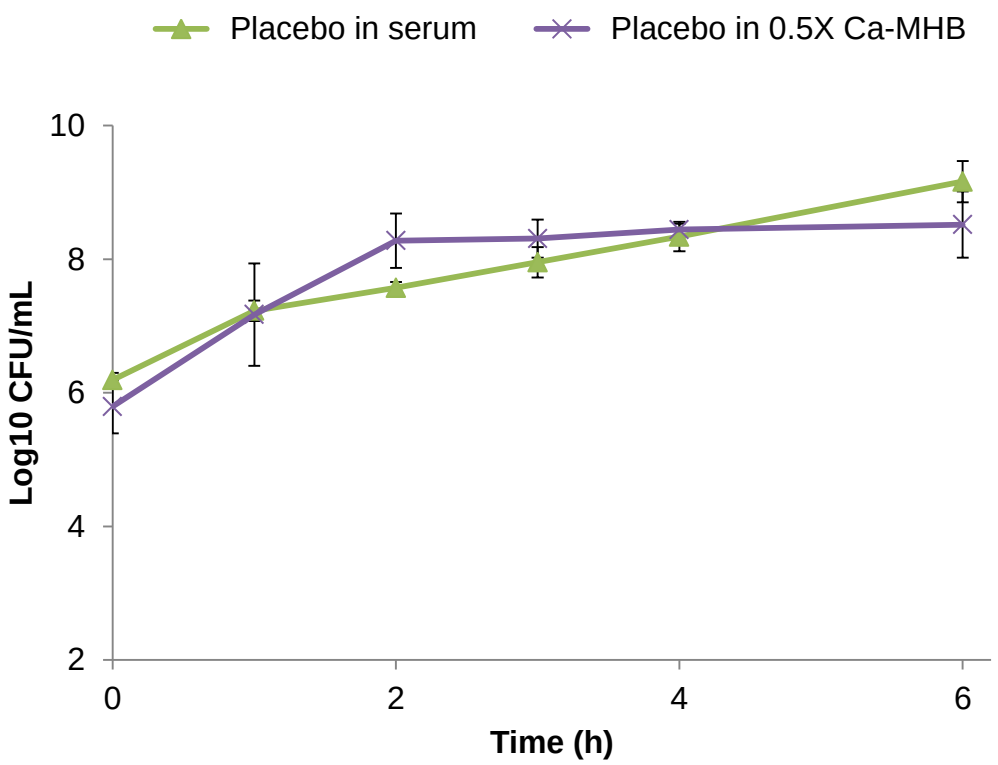

Figure 11: Time-kill results of minocycline in serum or 0.5X Ca-MHB

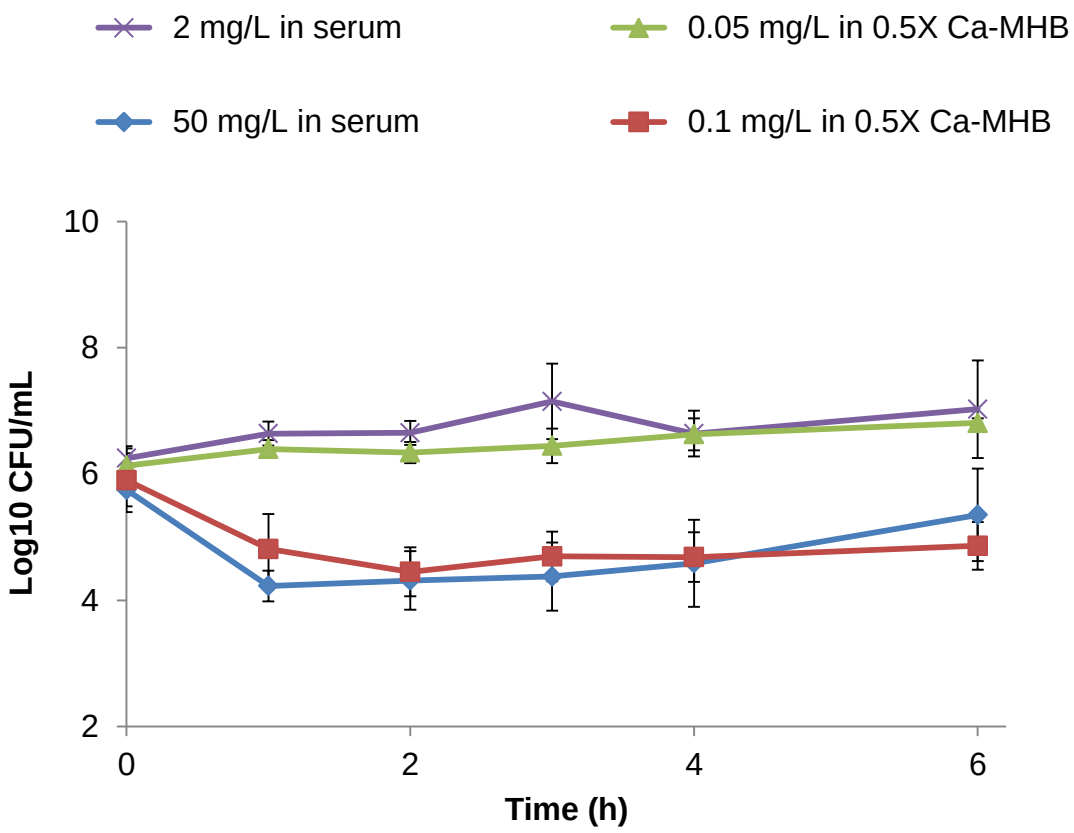

4.2.3 Minocycline pharmacokinetic study

The initial estimation of serum $AUC_{0\text{-}24h}$ and the best-fit C_{max} suggested that the pharmacokinetics of 25 mg/kg and 50 mg/kg doses were within the linear range. Also, the daily dose of 50 mg/kg was found to be comparable to the human equivalent AUC reported in a previous study (35). Therefore, the total daily dose was split into 5 doses to mimic a humanized regimen. Briefly, 18 mg/kg of minocycline was given at 0 h to achieve the serum C_{max} similar to that in humans, and 4 supplemental doses (11 mg/kg, 9 mg/kg, 8 mg/kg and 4 mg/kg given at 4 h, 9 h, 14 h and 22 h) were given to maintain the serum concentrations around the target pharmacokinetic profile reported in humans (18).

The data from these 3 dosing regimens were co-modeled, and PK parameters were shown in Table 3. The best-fit minocycline concentration-time profiles of different dosing regimens were shown in Figure 12. The profiles of minocycline in both serum (r^2 = 0.977) and ELF (r^2 = 0.952) were captured satisfactorily (as shown in Figure 13). The elimination half-life in serum was 2.6 h. The serum $AUC_{0\text{-}24h}$ were 34 mg*h/L, 68 mg*h/L and 63 mg*h/L for 25 mg/kg, 50 mg/kg and humanized regimen, respectively; while the ELF $AUC_{0\text{-}24h}$ were 94 mg*h/L, 189 mg*h/L and 175 mg*h/L. The pulmonary penetration ratio of minocycline was 2.8.

Compared to 50 mg/kg, the $AUC_{0\text{-}24h}$ of the 100 mg/kg dose observed was more than 3 times higher. Therefore, the concentration-time profiles of 100 mg/kg were analyzed separately (as shown in Figure 12), and PK parameters were shown in

Table 3. The r^2 were 0.971 and 0.867 for serum and ELF concentration-time profiles (as shown in Figure 13). The elimination half-life was prolonged (3.9 h), suggesting saturable clearance for the 100 mg/kg dose. The $AUC_{0\text{-}24h}$ were 227 mg*h/L and 564 mg*h/L for serum and ELF, respectively. The pulmonary penetration ratio was 2.5.

Table 3: Best-fit PK parameters

PK parameters	Group 1 (25, 50 mg/kg and humanized regimen)	Group 2 (100 mg/kg)
K_e (1/h)	0.27	0.18
V_c (L/kg)	2.7	2.4
K_a (1/h)	2.3	4.6
Pulmonary penetration ratio	2.8	2.5
$t_{1/2}$ (h)	2.6	3.9
CL (L/h/kg)	0.7	0.4

Figure 12: Minocycline serum and ELF concentration-time profiles

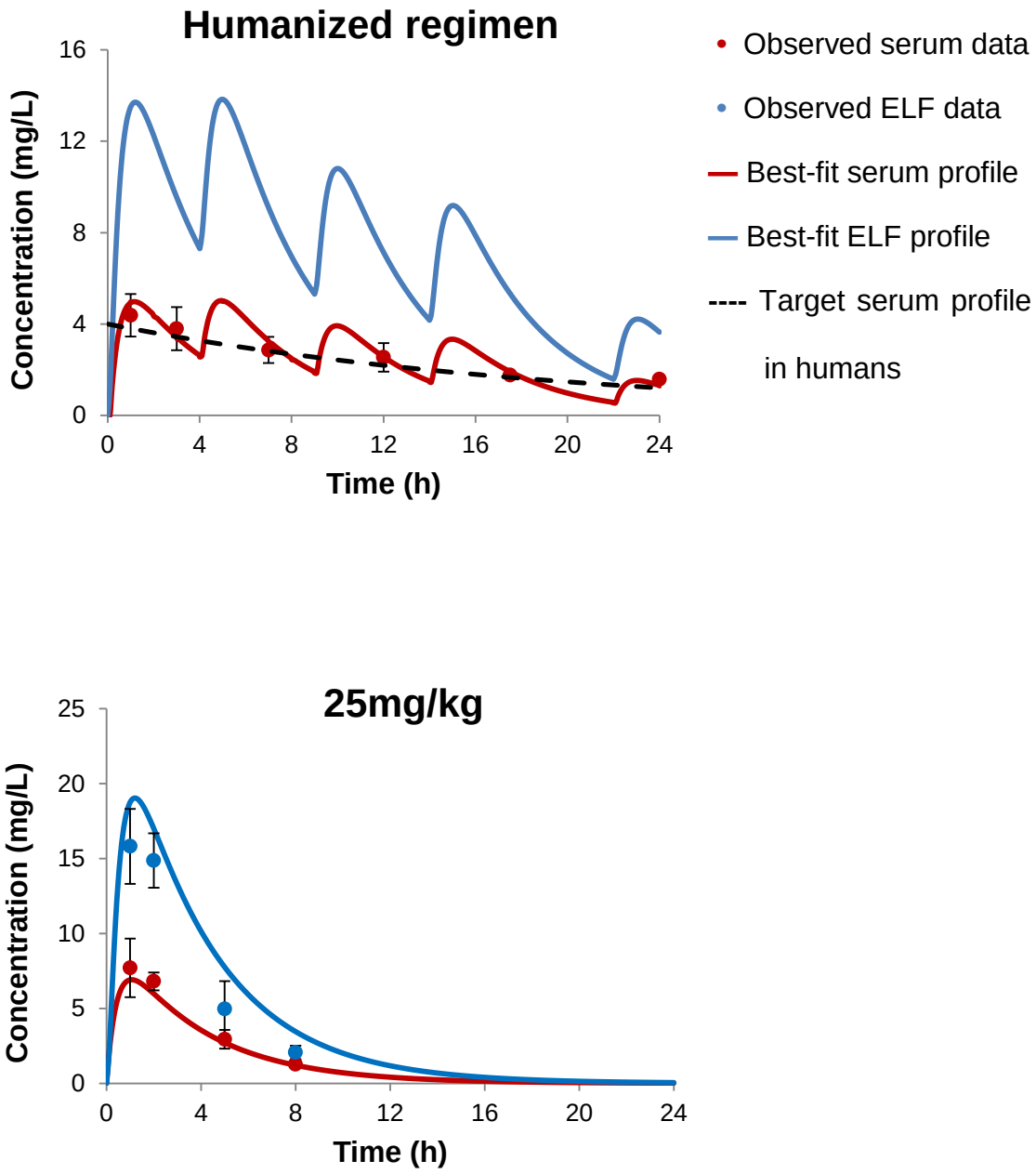

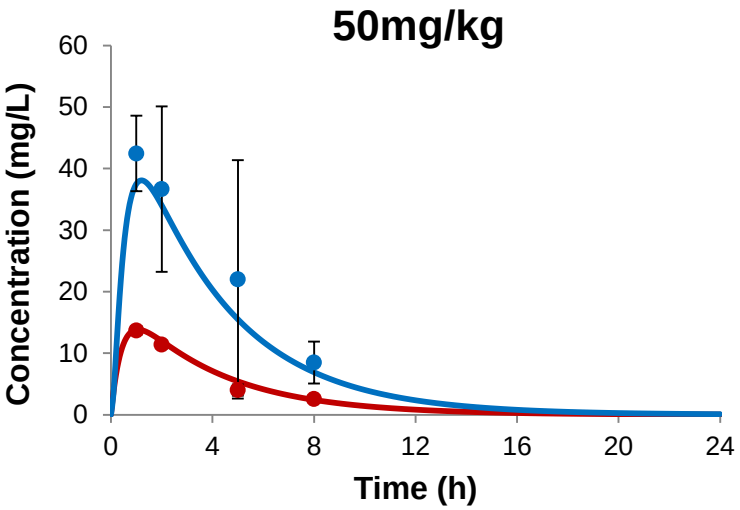

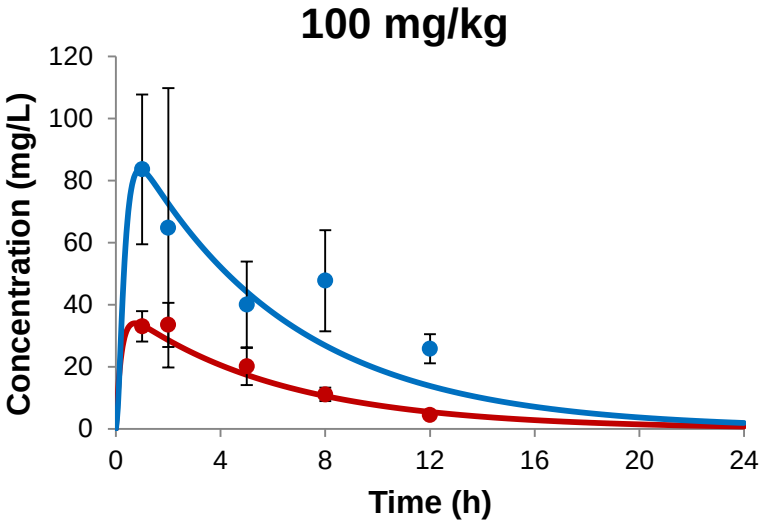

Note: The observed data were shown as mean ± SD.

Figure 13: Correlation between observed and best-fit PK data

A. 25 mg/kg, 50 mg/kg and humanized regimen

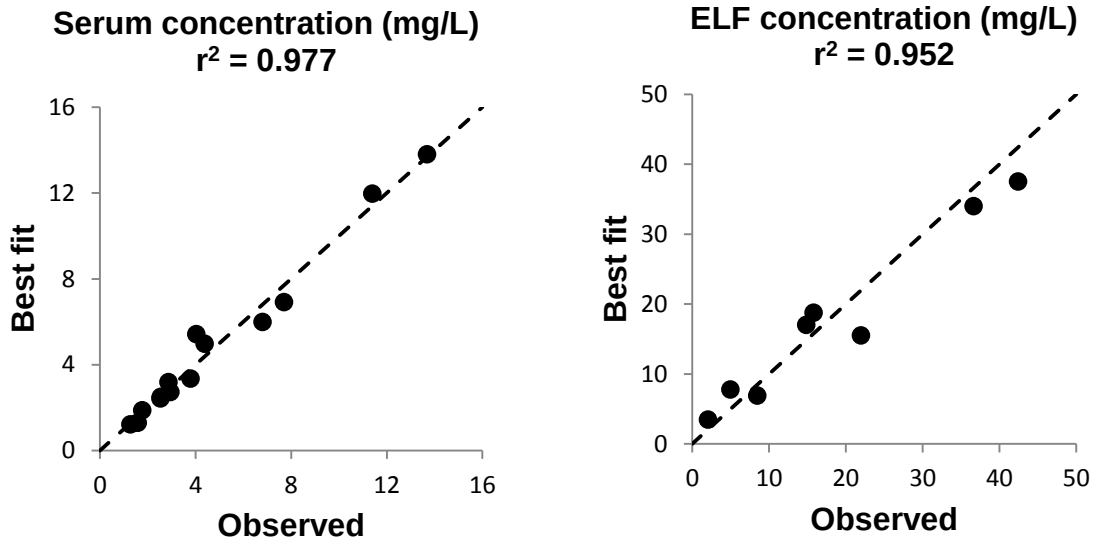

B. 100 mg/kg

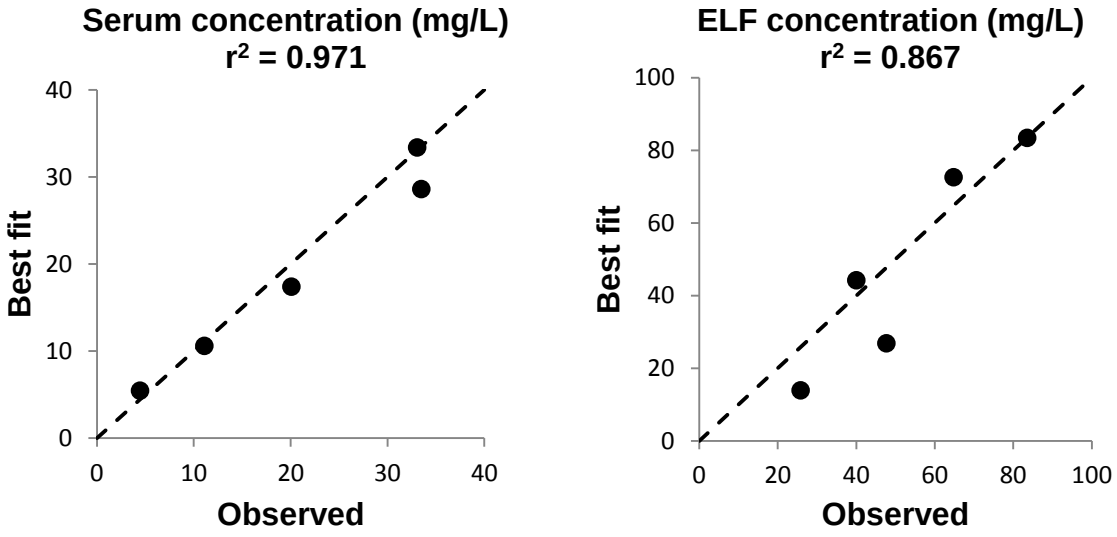

Note: The dashed line is the line of identity (i.e., y=x).

CHAPTER 5: MAXIMIZE MINOCYCLINE *IN VIVO* EFFICACY

To maximize minocycline *in vivo* efficacy, we need to explore the drug exposure-response relationship. Due to the complexity of serum protein binding, ELF exposure was used instead of systemic free drug exposure in the PK/PD modeling. Then the PK/PD magnitudes for different PD targets could be determined by the model.

5.1 Materials and methods

5.1.1 Materials

The Ultra Clean microbial DNA isolation kit was from Mo Bio laboratories, Inc. (Carlsbad, CA); DNA *Acinetobacter* strain typing kit was a product of Diversilab (Marcy l'Etoile, France), and Taq DNA polymerase was purchased from Bioline USA Inc (Randolph, MA). The urea assay kit was from BioAssay Systems (Hayward, CA).

5.1.2 Bacterial isolates

5.1.2.1 *In vitro* susceptibility

Five *A. baumannii* isolates (1 laboratory wild-type isolate and 4 clinical isolates) with a wide range of minocycline MICs were used. Susceptibilities to minocycline, doxycycline, amikacin and imipenem were determined by the broth dilution method as recommended by CLSI (as described in section 3.1.2.1).

Pseudomonas aeruginosa strain ATCC 27853 (American Type Culture Collection, Manassas, VA) was used as a control strain. In addition, the MICs of minocycline for 4 isolates were determined in the in the presence of phenylanine-arginine β-naphthylamide (PAβN) (100 mg/L), an efflux pump inhibitor (53). In order to exclude the inhibitory effect of PAβN, the bacterial burden of each positive control was determined by QC as described in section 3.1.1.

5.1.2.2 Clonal relatedness

The clonal relatedness of the *A. baumannii* isolates was assessed by repetitive-element–based polymerase chain reaction (rep-PCR) (54, 55). Briefly, genomic DNA was isolated using Ultra Clean microbial DNA isolation kit, and used as the template for the *Acinetobacter* strain typing kit. The PCR reaction was performed on 2720 Thermal Cycler (Applied Biosystems, CA). The AmpliTaq DNA Polymerase was used, and the total reaction volume was 25 µL. Parameters of Thermal Cycler was listed in Table 4. The DNA fragments of rep-PCR products were separated by the Agilent 2100 Bioanalyzer (Agilent Technologies, Santa Clara, CA), and compared by the DiversiLab software using the Pearson correlation coefficient (Bacterial Barcodes, Inc., Athens, GA).

Table 4: Parameters of AB 2720 Thermal Cycler

Steps	Temperature (°C)	Time (seconds)
Initial Denaturation	94	120
Denaturation	94	30
Annealing	50	30
Extension	70	90
Final Extension	70	180
Hold	4	-
Cycles	**35**	

5.1.2.3 Resistance mechanisms

Colony quantitative PCR (qPCR) was carried out to determine the presence of the *tetA*, *tetB*, *tetM*, and *tet39* genes in *A. baumannii* strains. Colonies of overnight-streaked strains on LB agar plates were chosen, resuspended, heated, and used as PCR templates. The qPCR was run using Sybr green Select master mix (ABI) in an ABI 7000 sequence detection system. The threshold cycle (C_T) values were normalized with the housekeeping gene *recA* of the same strain. The difference (ΔC_T) was used as a logarithmic power (base = 2) to calculate the relative signal of the gene. The transcription levels of the known efflux genes, *adeB*, *adeJ*, and *adeG*, were determined by reverse transcription (RT)-qPCR. Cells were grown in cation-adjusted Mueller-Hinton broth (Ca-MHB) and centrifuged, and total RNA was isolated (Ambion *RiboPure* Bacteria RNA isolation kit [ABI]). The RT reaction was performed using the TaqMan reverse transcriptase reagent kit (ABI) with a mixture of primers. The results (C_Ts) were normalized with the housekeeping gene *rpoB*.

5.1.3 Minocycline *in vivo* PD study

The mice were inoculated with approximately 10^7 CFU of *A. baumannii* isolate by the methods described in section 3.2. Infected animals were treated with different dosing regimens of minocycline about 2 h after infection. For reference, there was a no treatment control group for each bacterial isolate. There were 80 animals given 23 dosing regimen - bacterium combinations in total (n≥3 for each

regimen). For reference, there was a placebo (i.e., no treatment) control group for each bacterial isolate. The bacterial burdens in lung tissues were determined at 0h (baseline) and 24h after first dose of minocycline as described elsewhere (35, 56). Briefly, after the animals were sacrificed by CO_2 asphyxiation, the lung tissues were harvested and homogenized in sterile saline. Pulmonary bacterial burdens were determined by quantitative culture (as shown in section 3.1.1), and normalized by the weights of lung tissues.

5.1.4 Data analysis

The relationships between minocycline PK/PD indices (unbound drug exposures in ELF) and bacterial burden in lung tissues at 24 h were described by an inhibitory sigmoid E_{max} model (as shown in Figure 14) (40). The coefficient of determination was used to discriminate the PK/PD index most closely correlated to bactericidal activity. In addition, the best-fit parameters were also used to derive the required PK/PD magnitudes for maintaining stasis or achieving 1 log reduction of bacterial tissue burden at 24h.

Figure 14: Inhibitory sigmoid E_{max} model

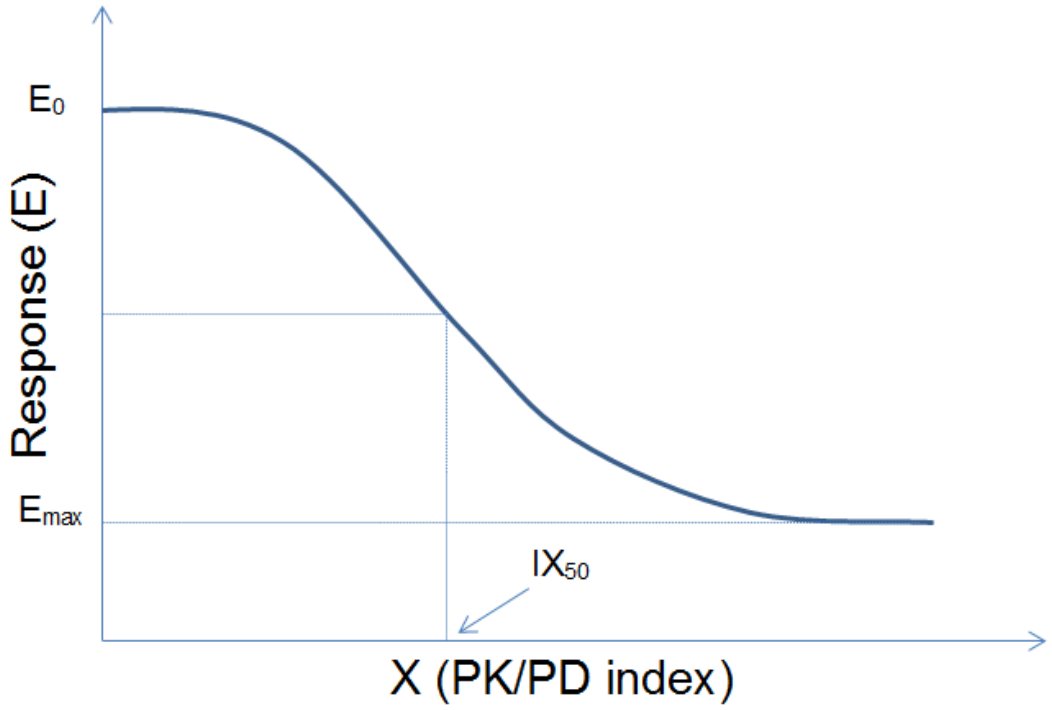

Inhibitory sigmoid E_{max} model: $E = E_0 - E_{max} \times X^H / (IX_{50}^H + X^H)$

E: PD response at 24h

E_0: the top of the curve

E_{max}: the maximum effect

X: the value of PK/PD index (ELF)

IX_{50}: the required value of X to achieve 50% of the E_{max}

H: the Hill slope of the curve

5.2 Results

5.2.1 Susceptibility and clonality assessment

The tetracycline resistance mechanisms and susceptibilities of the *A. baumannii* isolates to various antibiotics were shown in Table 5. No effects were attributed to the PAβN concentration used (data not shown). In the presence of PAβN, the MIC of AB7416 was not as low as those of the other strains. It is unclear if this is due to the presence of *tetB* or another, alternative mechanisms(s). Cross-resistance was observed between minocycline and doxycycline. The isolates were found to belong to 3 clonally diverse groups (as shown in Figure 15 below).

Table 5: Susceptibilities of *A. baumannii* isolates

Isolate	Source	Tetracyline resistance mechanism(s)	MIC (mg/L)			
			Minocycline /Minocycline+PAβN	Doxycycline	Imipenem	Amikacin
AB BAA 747	Laboratory	Wild-type	0.25/0.125	0.25	0.25	2
AB 7283	Clinical	Moderate overexpression of *adeB*	0.5/0.125	0.5	**128**	**128**
AB 1261	Clinical	Moderate overexpression of *adeB*	1/0.125	0.5	**128**	**128**
AB 1129	Clinical	*adeABC* and *adeIJK* overexpressed	4/-	4	**8**	**32**
AB 7416	Clinical	*tetB*, moderate overexpression of *adeB*	**16**/2	**128**	**16**	**> 512**

Note: Bold fonts depict resistant phenotype as defined by the Clinical and Laboratory Standards Institute (CLSI)

Figure 15: Dendrogram of *A. baumannii* clonality.

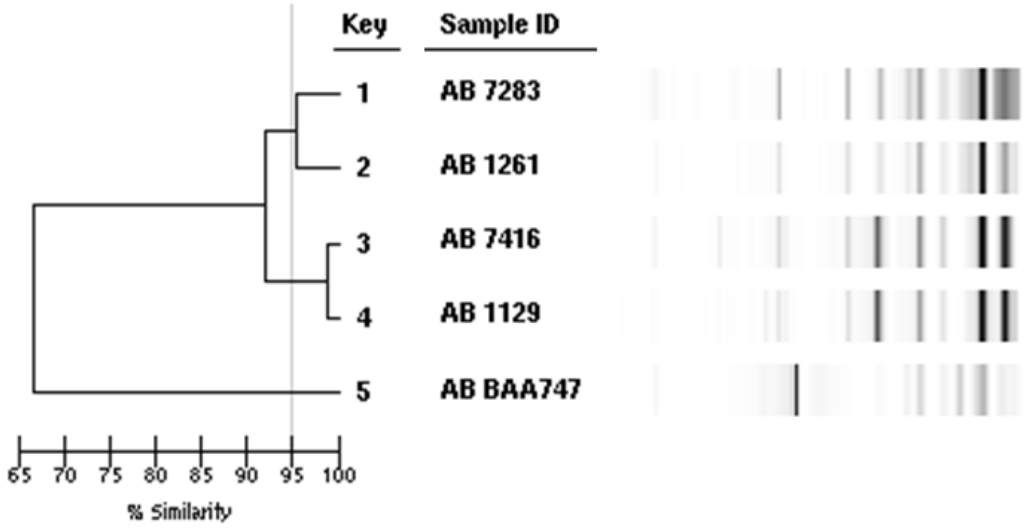

5.2.2 Minocycline *in vivo* PD study

The baseline bacterial burdens in lung tissues ranged from 7.75 to 8.18 log CFU/g. In the absence of treatment, the tissue burdens increased to 8.60 to 9.65 log CFU/g in 24h. All treatment groups infected with the minocycline-resistant isolate (AB7416) showed similar results as the no treatment control group, while the other susceptible / intermediate isolates were suppressed to various extents. Different dosing regimens with the daily dose of 50 mg/kg (i.e., 50 mg/kg single dose, 25 mg/kg every 12 h and humanized regimen) were given to mice infected with AB 7283, AB 1261 and AB 7416. For each isolate, there were no significant differences in bacterial burden at 24 h among these 3 dosing regimens. Therefore, ELF AUC/MIC should be the most appropriate PK/PD index for minocycline.

5.2.3 PK/PD correlation

According to the best-fit PK parameters, the PK/PD indices for ELF profiles of different dosing regimens against various *A. baumannii* isolates were calculated, and listed in Table 6. The relationships between minocycline PK/PD indices in ELF and bacterial tissue burden at 24h were shown in Figure 16. The strongest relationship was observed when the tissue burdens were correlated with $AUC_{ELF\ 0\text{-}24h}$/MIC (r^2 = 0.81). Using the best-fit parameters, the required $AUC_{ELF\ 0\text{-}24h}$/MIC for maintaining stasis was 140, and the required $AUC_{ELF\ 0\text{-}24h}$/MIC for achieving 1 log reduction was 410.

Table 6: PK/PD indices for ELF profiles of different dosing regimens against various *A. baumannii* isolates

AUC/MIC

	AB BAA 747	AB 7283	AB 1261	AB 1129	AB 7416
Placebo	0	0	0	0	0
25mg/kg	377	189	94	24	6
25mg/kg x 2	743	371	186	46	12
50mg/kg	755	377	189	47	12
Humanized	701	351	175	44	11
50mg/kg x 2	1478	739	369	92	23
100mg/kg	2258	1129	564	141	35

%T>MIC

	AB BAA 747	AB 7283	AB 1261	AB 1129	AB 7416
Placebo	0	0	0	0	0
25mg/kg	74	63	52	30	7
25mg/kg x 2	100	100	100	61	14
50mg/kg	85	74	63	41	19
Humanized	100	100	100	80	0
50mg/kg x 2	100	100	100	83	39
100mg/kg	100	100	100	81	46

C_{max}/MIC

	AB BAA 747	AB 7283	AB 1261	AB 1129	AB 7416
Placebo	0	0	0	0	0
25mg/kg	76.1	38.1	19.0	4.8	1.2
25mg/kg x 2	79.5	39.8	19.9	5.0	1.2
50mg/kg	152.2	76.1	38.1	9.5	2.4
Humanized	55.4	27.7	13.8	3.5	0.9
50mg/kg x 2	159.1	79.5	39.8	9.9	2.5
100mg/kg	333.6	166.8	83.4	20.8	5.2

Figure 16: Correlation of PK/PD indices in ELF and tissue burden at 24h

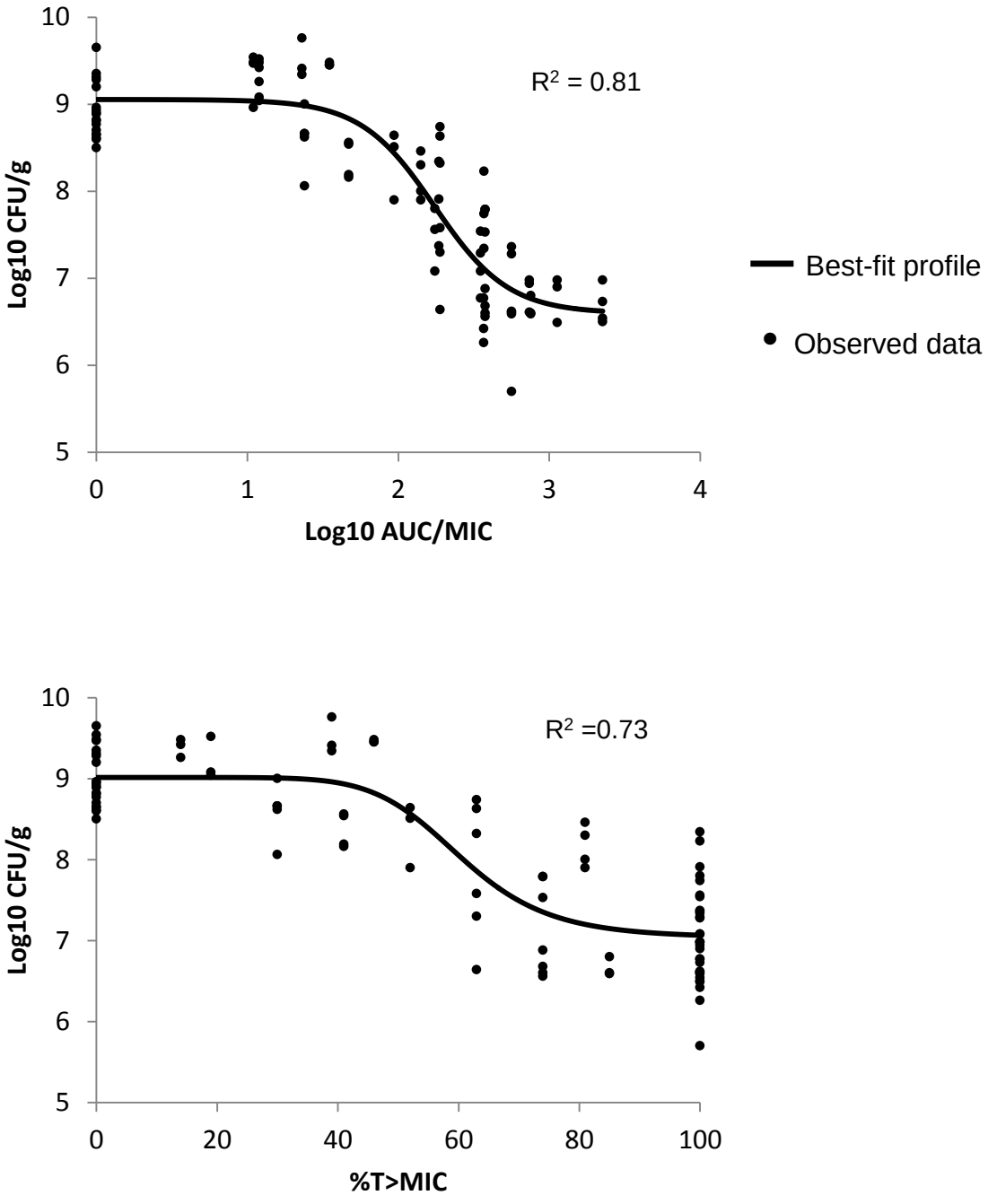

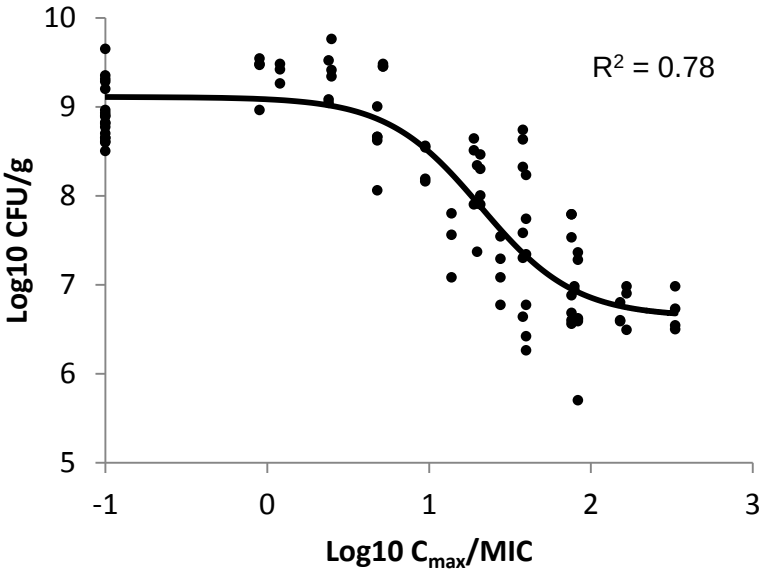

Each data point represents an observation from a single animal. In view of the logarithmic scale used, AUC/MIC values were input as 1 and C_{max}/MIC values were input as 0.1 for placebo controls.

CHAPTER 6: RESISTANCE DEVELOPMENT

To explore mechanisms of minocycline resistance development during therapy, resistant mutants of laboratory wild type strain AB BAA 747 were isolated from mouse lung tissue samples. In future, whole genome sequencing (WGS) will be used to identify mutant genes. In this chapter, the mutants were characterized to ensure clonal relatedness and stable susceptibility. Additional studies, such as cross resistance and growth rate, could provide more information for future studies about the resistance development mechanism.

6.1 Materials and methods

6.1.1 Resistant mutant preparation

The same neutropenic murine pneumonia model as described in section 3.2, was used for resistant mutant preparation. The mice were infected with approximately 10^7 CFU of AB BAA 747 (laboratory wild type isolate). A repeated dose of minocycline (25mg/kg) was administered everyday by intraperitoneal injection. The bacterial burdens in lung tissues were determined at 0h (baseline), 24h and 48h after the first dose of minocycline. Resistant mutants were isolated by plating lung tissue sample on Mueller-Hinton agar plates, which contain 2 times MIC of minocycline (0.5 mg/L). The plates were incubated at 37°C, and mutants of 48h samples were collected.

6.1.2 Mutational frequency

Mutational frequencies were calculated as the number of resistant mutants divided by the total bacterial burden. The *in vitro* baseline mutational frequency of AB BAA 747 was determined by inoculating approximately 10^9 CFU of bacteria on the minocycline-supplemented agar plates (2× MIC). Plates were incubated at 37°C, and the number of resistant mutants was determined after 48h. Mutants were collected for later susceptibility test. The inoculum was confirmed by quantitative culture as described in section 3.1.1. The sample was prepared in triplicate, and the experiment was repeated three times on different days. Finally, the average of mutational frequency values was reported. Similarly, the mutational frequencies of AB BAA 747 in mouse lung tissue samples were also determined.

6.1.3 Characterization of the mutants

6.1.3.1 Susceptibility and stability of mutants

The MICs of minocycline for AB BAA 747 resistant mutants were determined by ETEST as described in section 3.1.2.2. The parent isolate AB BAA 747 was used as a control. To verify the stability of the mutation, mutants were sub-cultured in drug-free Ca-MHB 5 times. The MICs of minocycline were determined again. In addition, the MICs of levofloxacin for all the mutants were also determined by ETEST.

6.1.3.2 Time growth

Time growth studies of AB BAA 747 and the mutants were performed in 216Dx UTI System (BacterioScan, MO). Briefly, each isolate was inoculated into Ca-MHB, and incubated at 37 °C water bath, until achieving the log phase. Bacteria were diluted to approximately 5×10^5 CFU/mL, and 2 mL of each was transferred into the cuvette. The run time of the time growth study was 90 minutes, and the sampling interval was 5 minutes. Reads of bacterial burden were calibrated for AB BAA 747. A first order kinetics equation was used to fit the collected data in ADAPT 5. The differential equation was as shown below. The confidence intervals of k_g were used to compare AB BAA 747 and the mutants.

$$\mathbf{dN(t)/dt = N(t)*k_g}$$

N(t): Size of bacterial population at time t;

k_g: growth rate constant.

6.1.3.3 Repetitive Sequence-based polymerase chain reaction

The clonal relatedness of the parent isolates and mutants was assessed by repetitive-element–based polymerase chain reaction (rep-PCR) as described in section 5.1.2.2. The procedure was modified due to the availability of reagents. Briefly, the PCR reaction was performed on ProFlex PCR system (Life

Technologies, Inc.). Primer was from the DiversiLab strain typing kit for Acinetobacter (BioMerieux, France). The GoTaq DNA Polymerase was used, and the total reaction volume was 25 µL. Parameters of PCR system were the same as that in Table 4. The DNA fragments of rep-PCR products were separated by the Agilent 4200 TapeStation system (Agilent Technologies, Santa Clara, CA). The high sensitivity D5000 tape was used, and AB 7416 was used as negative control.

6.1.3.4 Pulsed-field gel electrophoresis

Pulsed-field gel electrophoresis (PFGE) was used to further confirm the clonal relatedness of all the *A. baumannii* isolates. A previously published PFGE method for *A. baumannii* was modified in our study (57). Briefly, 3 mL of the overnight culture was centrifuged (3200×g, 4°C) for 15 minutes. The supernatant was discarded, and the pellet was re-suspended by 1mL cell suspension buffer (CSB: 100mM Tris-HCL, 10mM EDTA). The same volume of 1.6% low melting point agarose was mixed with the bacterial cell suspension, and the mixture was poured into mold to make insert plug. The plugs were incubated in 0.5mL cell lysis solution 1(CLS-1: 50mM Tris-HCL, 50mM EDTA, 2.5mg/mL lysozyme, 150mg/L proteinase K) at 37°C for 5h, and then moved into 0.5mL CLS-2 (0.5mM EDTA, 1% sarcosyl, 50mg/L proteinase K) at 55°C overnight. Plugs were washed with 5mL sterile ultra-pure water at 55°C for 15 minutes (3 times), and

then washed similarly by Tris-EDTA (TE). The plugs could be stored in TE buffer at 4°C for up to 2 years.

*Apa*I endo-nuclease enzyme (New England Biolabs, MA) was used for restrictive digestion of genomic DNA (30U/sample). Plugs were incubated at 25°C overnight, washed with pure water, and then incubated in TE at 37°C for 1h. The PFGE gel consisted of 1.6% I.D.NA agarose (Lonza, Switzerland). DNA fragments were separated by a CHEF-DR III system (Bio-Rad Laboratories, Belgium) at 14°C, with 6 V/cm^2 for 24h. The initial and final switch times were 2s and 28s, respectively. The gel was stained with 5µg/mL ethidium bromide for 20min, and then de-stained in pure water for 30min. The results were visualized under UV lights.

6.2 Results

6.2.1 Mutational frequency

The *in vitro* baseline mutational frequency of AB BAA 747 was 2.3×10^{-7}. Ten mutants were randomly collected, and all of them showed elevated MIC of minocycline (≥3 times). After being passed 5 times in drug-free Ca-MHB, nine of them still showed stable susceptibility to minocycline (data is not shown here).

For animal studies, increased average mutational frequency was observed, when mice were administered 25mg/kg/day minocycline. The mutational frequency

over time was shown in Figure 17. Nine resistant mutants were collected from 3 mice at 48h.

Figure 17: Mutational frequency of AB BAA 747 collected from lung tissue samples

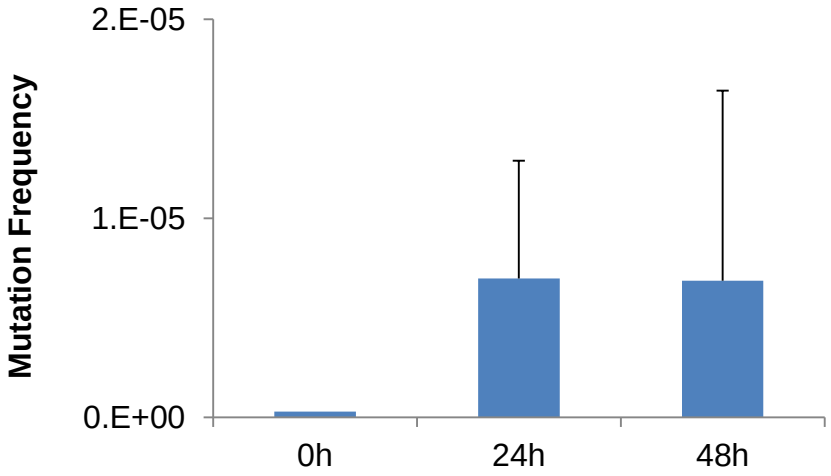

6.2.2 Characterization of mutants

6.2.2.1 MIC and stability of mutation

The MICs of minocycline for AB BAA 747 and its mutants were shown in Table 7. Compared to the parent isolates, seven out of nine isolates were observed elevated MIC (≥3 times). After being sub-cultured in drug free Ca-MHB for 5 times, all the mutants showed stable elevated MIC. The susceptibilities of mutants to levofloxacin were also shown in the table, and two of the mutants showed cross-resistance between minocycline and levofloxacin.

Table 7: Susceptibility and stability of the mutants

Strain	Minocycline MIC (mg/L)	Minocycline MIC after 5 days (mg/L)	Levofloxacin MIC (mg/L)
AB BAA 747	0.25	0.5	0.25
Mutant 1	1.5	2	0.19
Mutant 2	1.5	2	0.19
Mutant 3	1.5	1.5	0.19
Mutant 4	1.5	1.5	0.75
Mutant 5	1.5	2	0.19
Mutant 6	1.5	1.5	0.19
Mutant 7	0.25	0.38	-
Mutant 8	2	2	0.75
Mutant 9	0.25	0.38	-

6.2.2.2 Time growth

Seven mutants with elevated MICs were included in time growth study. Three out of seven isolates grew significantly slower than the parent isolate. The results were shown in Figure 18, and the growth rate constants were shown in Table 8.

Figure 18: Time growth results of AB BAA 747 and the mutants

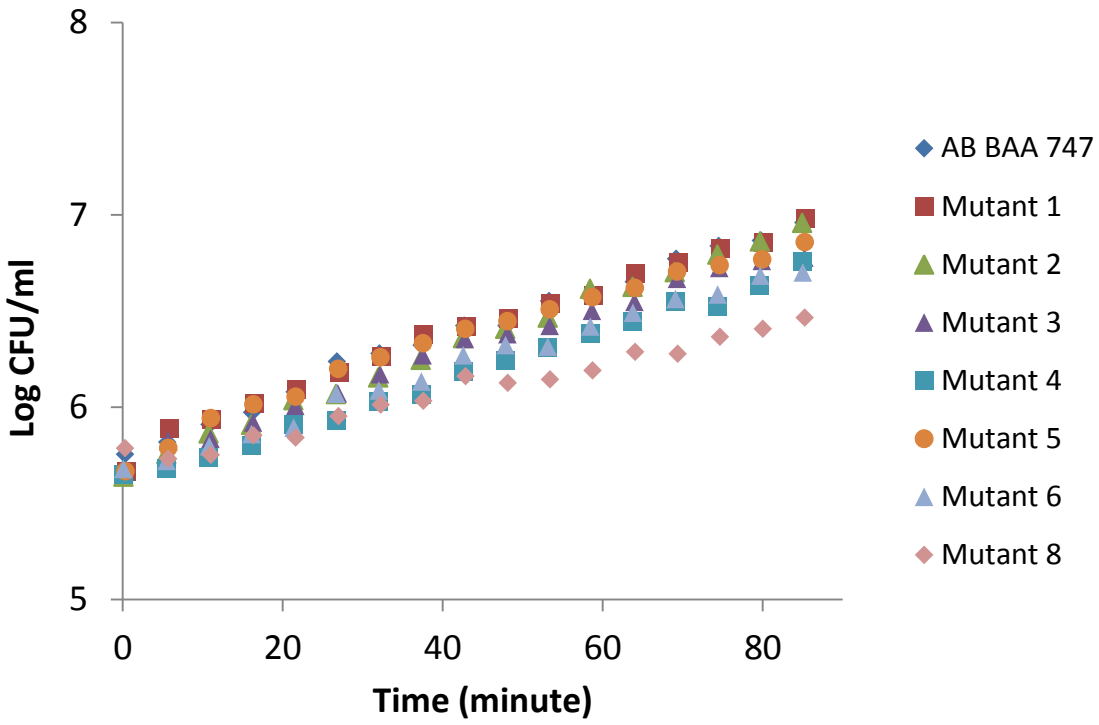

Table 8: Growth rate constants of AB BAA 747 and the mutants

	k_g (1/h)	95% confidence interval of k_g		r^2
		Low	High	
AB BAA 747	1.854	1.743	1.965	0.993
Mutant 1	1.86	1.746	1.974	0.993
Mutant 2	2.029	1.937	2.121	0.996
Mutant 3	1.636	1.493	1.779	0.985
Mutant 4	1.842	1.683	2.001	0.985
Mutant 5	**1.576**	**1.47**	**1.682**	**0.991**
Mutant 6	**1.618**	**1.503**	**1.733**	**0.990**
Mutant 8	**1.214**	**1.112**	**1.315**	**0.983**

6.2.2.3 Repetitive Sequence-based polymerase chain reaction

Mutant 8 was excluded from this step due to the impurity of the isolate. The results of rep-PCR products in TapeStation were shown in Figure 19. All the mutants showed a pattern similar to that of AB BAA 747, and AB7416 showed different patterns.

Figure 19: Results of rep-PCR products in TapeStation

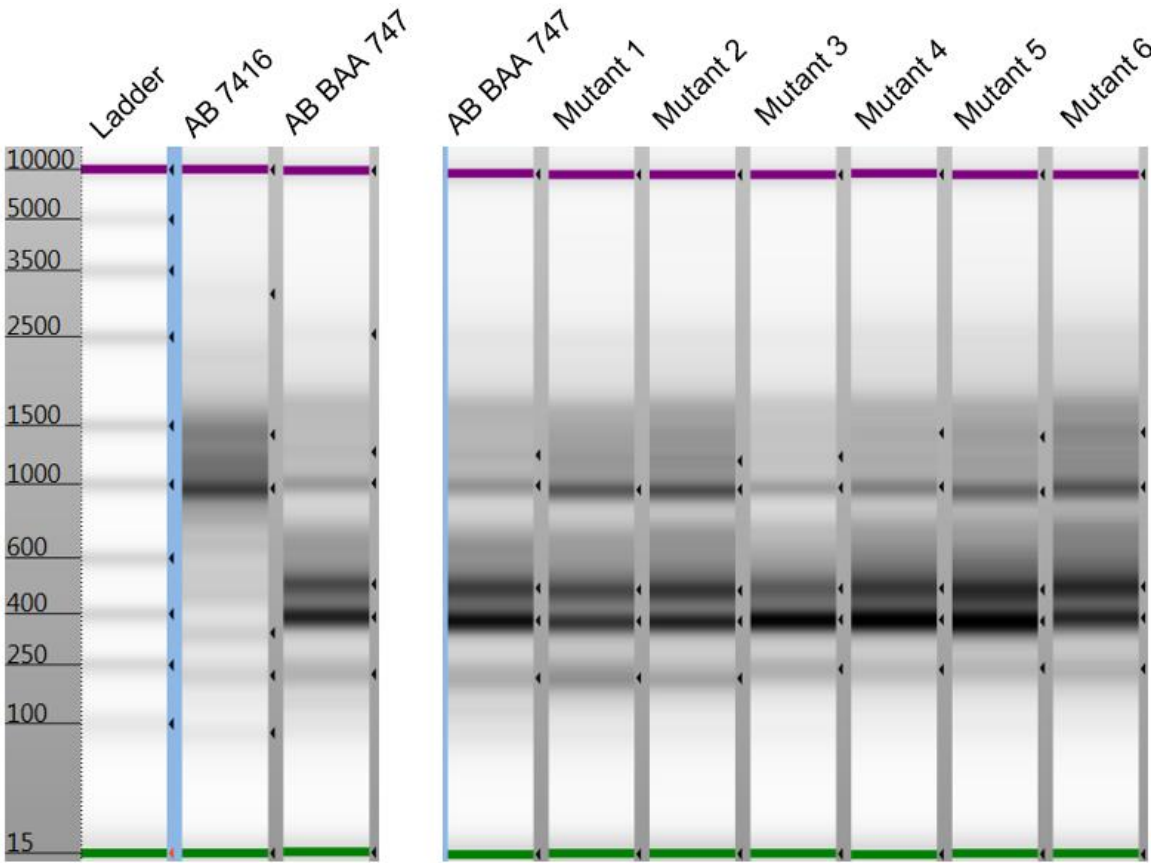

6.2.2.4 Pulsed-field gel electrophoresis

The Photo of PFGE gel was shown in Figure 20. The tested isolates showed similar patterns of bands. Compared to AB BAA 747, only 1 additional band was observed for mutant 3 and 5.

Figure 20: Results of pulsed-field gel electrophoresis

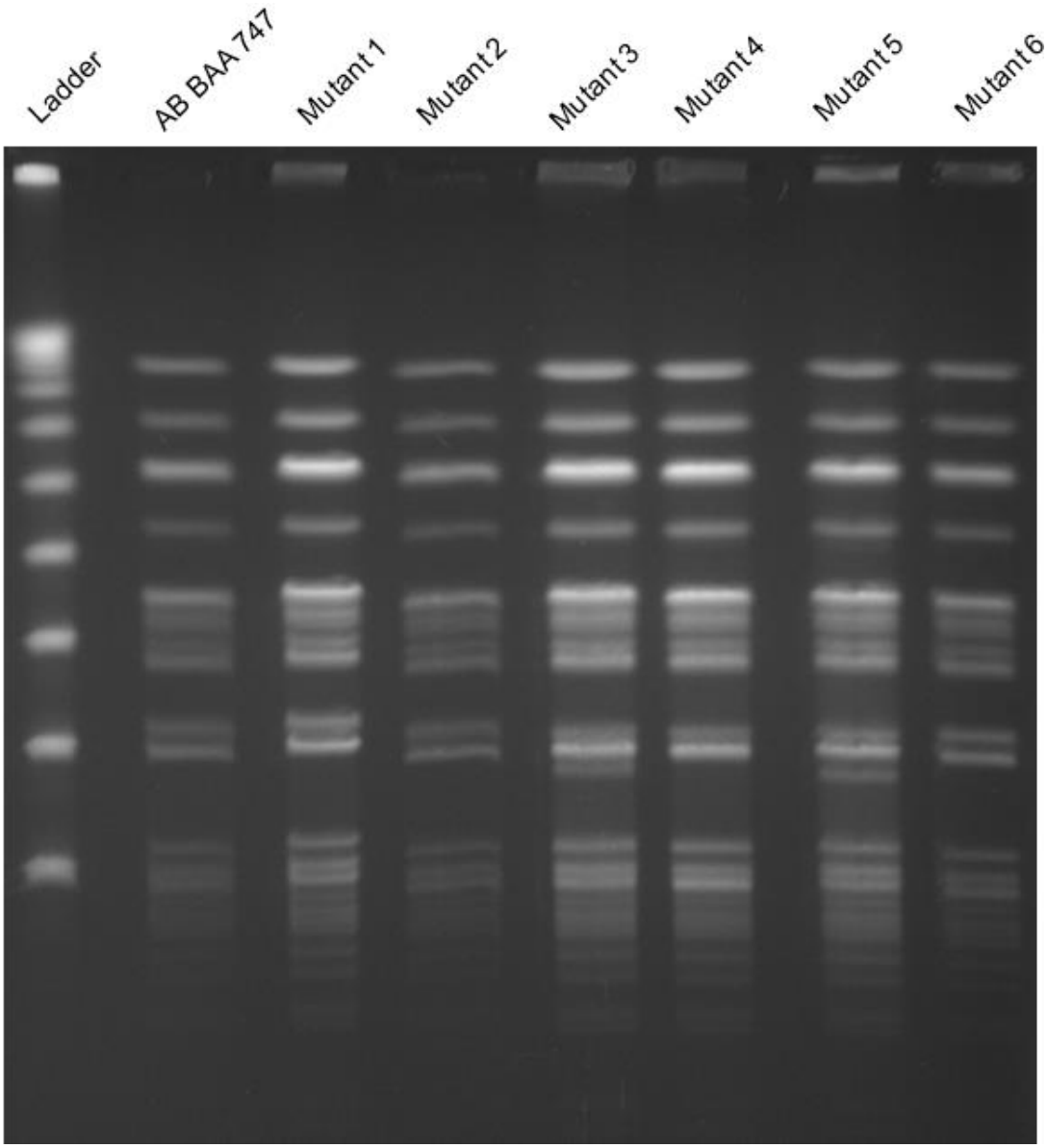

CHAPTER 7: CONCLUSIONS

7.1 Serum protein binding

Tigecycline and eravacycline were previously reported to have atypical non-linear serum protein binding; the free fraction decreased with increasing total concentration. In this study, we extended the investigations to other tetracyclines and examined if this could be a generalized class effect.

Although serum protein binding is known to play an important role in PK and PD of drugs, no standard method has been established yet. There are various methods available for determining serum protein binding, such as equilibrium dialysis, ultrafiltration, microdialysis, ultracentrifugation, fluorescence spectroscopy as well as chromatography and capillary electrophoresis (58). In addition, *in vitro* time-kill study could provide functional validation of the serum protein binding, although it is not as accurate as the analytical chemistry approaches (49). Usually, equilibrium dialysis is considered as the “reference method”， because it is more precise than other approaches (59, 60). However, it is time-consuming and labor-intensive. In contrast, microdialysis shares similar mechanism with equilibrium dialysis, but requires less time. The system has been well established, and been described in many papers (26, 61-63).

In the current study, within a clinically achievable concentration range, minocycline and doxycycline were found to have the same trend of protein

binding as tigecycline. The atypical non-linear protein binding appears consistent across several tetracyclines. Serum protein binding of minocycline is usually accepted as 76% (determined by ultrafiltration) (23), and is similar to our results using PBS with a low minocycline concentration. If the atypical non-linear protein binding is confirmed, the use of tetracyclines for the treatment of bacteremia should be re-evaluated. This is especially relevant for pathogens with low to intermediate-level resistance, as higher doses may not yield better therapeutic outcomes. The exact mechanisms of the atypical non-linear protein binding is not clear, Singh RS et al. suggested that it could be caused by chelating effect of tetracyclines to divalent metal ions (29). The addition of ethylenediaminetetraacetic acid (EDTA) resulted higher unbound fraction, and the atypical profile disappeared. Moreover, our results also suggested that different perfusion media used might also have an impact on the microdialysis results. Therefore, specific conditions of the microdialysis experiments require further optimization / standardization. Correlating the results from *in vitro* systems to *in vivo* microdialysis should also be considered (64).

In addition, time-kill studies with different minocycline concentrations in mouse serum or 0.5X Ca-MHB were used as functional validation of minocycline serum protein binding. Although, calculated protein binding values were higher than that derived by microdialysis, the observed trend of nonlinear serum protein binding was same as that in microdialysis studies. When minocycline concentration in

0.5X Ca-MHB increased from 0.05 to 0.1 mg/L, the comparable minocycline concentration in serum increased from 2 to 50 mg/L.

In summary, serum protein binding of minocycline is atypically concentration-dependent. In addition, the microdialysis results could vary considerably when different perfusion media are used. To understand the mechanism(s) and clinical implications of serum protein binding to minocycline, additional studies are warranted.

7.2 Pharmacokinetics of minocycline

Because of high lipophilicity, about 95%-100% of orally administered minocycline could be absorbed, and it has the highest penetration into organs among all the tetracyclines (65). In the current study, minocycline exposure in ELF was higher than systemic total drug exposure (2.5-2.8×). In the treatment of pneumonia, this property will lead to drug accumulation in the site of infection. Although the distribution of minocycline in humans ELF has not been reported, the ratio of minocycline concentrations between bronchial secretions and blood was studied before. However, the results were not consistent from one study to another, and the values ranged from 0.3 to 2.2 (23, 65-67). To optimize dosing regimen of minocycline in humans, a better understanding of the bio-distribution is required. Therefore, more data of minocycline bio-distribution in humans is desired.

The PK parameters of minocycline in animals and humans have been studied previously. In horses, the elimination half-life was 7.7 ± 1.9 h (mean ± SD) after a 2.2 mg/kg single IV injection (68). A prolonged half-life (11.5 ± 3.2 h, mean ± SD) at steady state was observed when the dose was increased to 4 mg/kg q12h (69). The observation of non-linear pharmacokinetics reported with high doses was consistent with our findings from the current study (100 mg/kg in mice), and might be due to saturation of drug metabolism (70). Minocycline has variety of metabolites in humans. Two mono-N-demethylated derivatives and 9-hydroxyminocycline were reported to be the major metabolites (70). With API5500 Qtrap triple quadrupole mass spectrometer, the same metabolites have been identified in mouse serum PK sample too (data not shown in here). The elimination half-life in humans ranged from 12 h to 18 h, and the $AUC_{0-\infty}$ of serum concentration-time profile were 70-86 mg*h/L after 200 mg was given intravenously (18). Only 8-20% of the dose was recovered from human urine (65, 71). Therefore, little increase of elimination half-life was observed in renal impaired patients (72, 73). Up to 800 mg of minocycline daily has been given intravenously in a clinical trial for acute spinal cord injury (21), however there is little known to date about the dose linearity of minocycline in humans. A prospective study examining the safety, tolerability, and pharmacokinetics of minocycline (single and multiple ascending doses) in heathy adults has been planned (ClinicalTrials.gov identifier: NCT02802631). In clinically achievable

dose, if the non-linear clearance of minocycline was also observed in humans, better therapeutic outcomes are expected due to the extra drug exposure.

In conclusion, the pharmacokinetics of minocycline in mice serum and ELF were characterized. These findings could facilitate subsequent PK/PD study of minocycline for infections caused by *A. baumannii*.

7.3 Exposure-response relationship of minocycline

The shortage of new effective antibiotics against MDR *A. baumannii* prompted us to maximize the effectiveness of the currently available drugs, such as minocycline. With a good understanding of the drug exposures and bacterial susceptibilities likely to be encountered, a PK/PD model could facilitate the optimal use of minocycline. *In vitro* susceptibility results of minocycline are promising. Denys et al. reported the susceptibility data of Gram-negative bacteria from the U.S. between 2005 and 2011. In that study (n=883), the susceptibility rate of MDR *Acinetobacter* isolates to minocycline was 72.1 %, whereas most of other drugs examined were found to be resistant (10). Therefore, we want maximize minocycline *in vivo* efficacy by exploring the exposure-response relationship.

Free drug exposures in serum are commonly used in PK/PD studies. In the current study, we found that minocycline concentrations in ELF were higher than those observed in the serum. Subsequently, the PK/PD analysis was performed

with unbound minocycline concentrations in ELF (i.e., the site of infection), as they were deemed to be more relevant to therapeutic outcomes of pneumonia. Furthermore, serum protein binding of the tetracyclines may not be as straight forward as one might anticipate. Tigecycline was previously shown to exhibit atypical serum protein binding; the fraction of binding was higher with increasing total drug concentration in serum (26). The serum protein binding of minocycline was found to be dependent on the experimental conditions. Microdialysis data suggested that protein bindings of minocycline in human and mouse sera were comparable at different concentrations (results shown in Figure 8). Since the ELF exposure of minocycline achieved in humans after a clinical dose is not available, the total drug concentration-time profiles in the serum was mimicked and we assumed pulmonary penetration ratios of minocycline in humans and mice were similar.

The first step of PK/PD modeling was to determine the most appropriate PK/PD index for minocycline. As we discussed in section 2.3, there are three commonly used PK/PD indices: C_{max}/MIC, %T>MIC and AUC/MIC. Dose fractionation study could help determining the best PK/PD index for antibiotics. Briefly, the same daily dose could be designed into different regimens. The most appropriate PK/PD index is determined by comparing the PD response: 1) If the PD response of different regimens are similar, we should choose AUC/MIC; 2) If the PD response of the single dosing regimen is the best, Cmax/MIC is the best PK/PD

index; 3) If the PD response of the most frequent regimen is the best, the PD/PD index should be %T>MIC. In the current study, we used 3 different bacterial isolates, and the regimens with the same daily dose (50 mg/kg single dose, 25 mg/kg every 12 h and humanized regimen) showed similar *in vivo* efficacy (data not shown here). Since these dosing regimens have similar $AUC_{0\text{-}24h}$ but different C_{max} and %T>MIC, $AUC_{ELF\ 0\text{-}24h}$/MIC was expected be the PK/PD index best correlating to the bacterial burden. The subsequent study was tested with 5 *A. baumannii* isolates. Using a wide range of minocycline exposure and bacterial susceptibility (23 dosing regimen – bacterium combinations in total), our initial finding was substantiated by the results of the full PK/PD analysis (as shown in Figure 16).

The PK/PD model described the relationship between minocycline exposure and bactericidal activity quantitatively. Maximum efficacy observed was approximately 1.5 log reduction of bacterial burdens from baseline. The required $AUC_{ELF\ 0\text{-}24h}$/MIC values for maintaining stasis or achieving 1 log reduction of bacterial tissue burdens were also estimated. $AUC_{ELF\ 0\text{-}24h}$ of humanized regimen (a clinical dose of 200 mg is given intravenously to humans) was 175 mg*h/L. With a MIC of 0.25 mg/L, the corresponding $AUC_{ELF\ 0\text{-}24h}$/MIC (700) is expected to achieve more than 1-log kill. However, the therapeutic outcomes will vary when the MICs are different. Using these estimates, minocycline dosing regimens could be optimized when the susceptibility of an *A. baumannii* isolate is

known. Furthermore, it is also important to avoid selective amplification of the resistant subpopulation(s) during treatment. In the future, additional studies are warranted to evaluate resistance development during therapy, and correlating minocycline exposures to therapeutic outcomes of patients with infections caused by *A. baumannii*.

In conclusion, we have identified threshold target exposures for achieving different PD responses in *A. baumannii* infections, and the information could be used to optimize minocycline dosing regimens.

7.4 *In vivo* resistance development

Increased mutational frequencies were observed for AB BAA 747 at 24h and 48h after the first dose, when mice were administered 25mg/kg/day. Six of the mutants isolated from mouse lung tissue samples had elevated MICs of minocycline. Cross resistance was observed for two of the mutants (mutant 4 and 8) between minocycline and levofloxacin, which suggests the existence of multi-drug efflux pumps over expression. To further confirm this hypothesis, quantitative PCR could be used to compare expression of *adeABC* and *adeIJK* (15, 16).

The clonal relatedness of the parent isolate and the mutants were determined by rep-PCR and PFGE. Both the results suggested that the selected mutants belonged to the same clonal family of AB BAA 747. The rep-PCR products of AB

isolates were previously separated by Agilent 2100 Bioanalyzer system, as described in 5.1.2.2. Due to the availability of reagents for Bioanalyzer, the Agilent 4200 TapeStation system was used. In rep-PCR study, the observed band patterns were the same for all the isolates. In PFGE study, only two mutants (mutant 3 and 5) were found to have one additional band, and the rest of the mutants had the same band pattern as AB BAA 747. According to the previously published criteria, AB BAA 747 and the mutants could be considered as “closely related” (74). There are several reasons that could cause changes in PFGE pattern: 1) The additional DNA fragments might be contributed by plasmid (75); 2) Genomic DNA may gain extra restriction sites, therefore some of the larger DNA fragments were broken into smaller fragments (76); 3) Similarly, loss of curtain genes that contain restriction sites could also change the PFGE patterns (77). Compared to AB BAA 747, only mutant 5 showed significantly slower growth rate. Mutant 3 also had decreased growth rate, but the difference was not significant. Both of them did not show cross resistance to levofloxacin, which suggested that the mutation did not involve over expression of multi-drug efflux pumps.

Better understanding of the functions that controlled by the mutant genes could help us optimize the regimen of minocycline, and then suppress resistance development in *A. baumannii*. In future, these isolates will be analyzed by whole genome sequencing to identify the mutant genes. Among all the isolates, mutant

5 should be the first choice, because it had the most different phenotypes from the parent isolate. We expect mutant 5 will give us more information about the mechanisms of resistance development.

CHAPTER 8: FUTURE DIRECTIONS

The minocycline serum protein binding was determined in the current study. Because of its complexity, we only confirmed the atypical non-linear serum protein binding of minocycline. It was found that different perfusion media applied in the microdialysis system could affect the results, and none of the results matched that of time-kill studies. To confirm the serum protein binding of minocycline, further studies are needed. Microdialysis could be used *in vivo* as well as the *in vitro* system (64). The previously described rat portal vein and jugular vein intubation model might be used for our future studies (78, 79). The simultaneous dialysate samples could be taken with the blood samples, and quantified by LC-MS/MS. This approach could eliminate the differences between *in vitro* and *in vivo* systems, and provide more accurate results.

The exposure-response relationship of minocycline for *A. baumannii* has been demonstrated in our studies, and the resistant mutants of AB BAA 747 have been isolated from mouse lung tissue sample. The stability of susceptibility and clonal relatedness for the six mutants have been confirmed. In future, these mutants could be used for studying the mechanisms of minocycline resistance development. The whole genome sequencing (WGS) technology will be applied to identify the mutant genes. Briefly, genomic DNA of selected resistant mutants and AB BAA 747 will be extracted. Genomic DNA of all strains will be fragmented and sequenced as paired-end reads on the HiSeq sequencing system (Illumina,

San Diego, CA, USA). Contigs will be determined by analyzing the raw genome sequence, and the reads will be aligned to the reference genome using Seqman by DNAStar. The SNPs (single nucleotide polymorphisms) and gene deletions will be identified by comparing the sequences.

As discussed in section 1.1, the elevated MIC of minocycline for *A. baumannii* might be caused by up-regulation of efflux pumps (*tetA, tetB*, *adeABC* and *adeIJK*, etc.) or ribosomal protection (*tetM*). The collected isolates may contain the mutant genes above, or other unknown mechanisms. The WGS results will reveal the genomic alternations of the mutants. If the functions of mutant gene(s) have been reported previously, it could be identified using BLAST (basic local alignment search tool) algorithm. Therefore, the gene(s) could be linked to reported resistance mechanism(s), and the gene(s) could be further confirmed by quantitative PCR. If the function of the identified gene(s) is unknown, editing the target gene (e.g. knocking in or out the gene) in mutants could help us understand the mechanisms. It is also possible that the development of resistance cannot be identified by mutational changes in DNA, but rather in the transcriptional changes of the derivatives (80). Comparative transcriptome analysis (by RNA sequencing) may be necessary.

The information obtained could guide modification of treatment strategy (dose adjustment or combination therapy). Although the typical regimen of minocycline in adults is 200 mg/day, up to 800 mg/day has been given intravenously in a

clinical trial for acute spinal cord injury (21). Therefore, a higher dose of minocycline might be used to improve therapeutic outcomes. Current treatment strategies for MDR *A. baumannii* include a combination of tigecycline, minocycline, carbapenems, polymyxins, and daptomycin (81-84). However, the rationales of selecting certain antibiotics for combination therapy were not well established. According to our previous study, compared to monotherapy, combination of minocycline and polymyxin B could improve therapeutic outcomes of pneumonia caused by *A. baumannii* (35). In that study, we hypothesized that polymyxin B could disrupt the cell membrane and the proper functioning of the efflux pumps, thereby enhancing the activity of minocycline. Increased intracellular minocycline concentrations were also observed when *A. baumannii* was exposed to polymyxin B. This study is an example of designing combination therapy based on the resistance mechanism. In future, with more information provided by WGS, we may discover more relevant mechanisms, and more treatment strategies could be considered for improving therapeutic outcomes of infections caused by *A. baumannii*.

The antibiotics from the same family share similar chemical, structural and antimicrobial mechanisms. Cross-resistance is usually observed for antibiotics from the same family. Therefore, we expect that the knowledge of minocycline could also be extended to other tetracyclines, and we will have more choices when treating infections caused by *A. baumannii*.

CHAPTER 9: CONTRIBUTION TO SCIENCE

In this project, we characterized the pharmacokinetics of minocycline in neutropenic murine pneumonia model, and then explored the *in vivo* exposure-response relationship of minocycline for infections caused by *A. baumannii*. One resistant mutant was selected for future resistance development mechanisms study.

The LC-MS/MS method developed for various antibiotics in our study was rapid, robust and sensitive. The run time for each sample was 5 minutes, including enough equilibration time between injections. The standard curve showed very good linearity within the clinical relevant serum concentration range, and only 10 µL of serum was needed for each sample. This method could be applied to clinical PK samples too, and it will considerably reduce the required amount of blood samples from patients. In addition, more antibiotics from various classes could be analyzed by the same method, and some of them have been validated (85).

The atypical nonlinear plasma protein binding of tigecycline and eravacycline has been reported before. Our studies confirmed that minocycline and doxycycline had the same trend of protein binding, which suggested that it could be a class effect of tetracyclines. In that case, we need to be cautious when using tetracyclines for septicemia caused by intermediate susceptible bacteria, as

increased doses may not result higher systemic free drug exposure. Meanwhile, we found that different perfusion media in the microdialysis system could give us different results. This property may not be important to the drugs with low serum protein binding. However, it is critical to drugs like minocycline, because the free portion could be around 6 folds different when using different perfusion media (typical C_{max} of minocycline in humans is 4 mg/L after 200mg IV bolus injection). It will remarkably increase the difficulty of projecting effective dosing regimens for humans. Therefore, standardized method is needed in future to make results from different protein binding studies comparable.

Because of promising *in vitro* efficacy, minocycline became a choice for patients infected with MDR *A. baumannii*. However, the *in vivo* efficacy has not been well established. The PK/PD model developed in our studies delineated the *in vivo* exposure-response relationship of minocycline for infection caused by *A. baumannii*. Usually, systemic drug exposure is used in PK/PD modeling for antibiotics. However, we used a modified PK model to describe drug exposure in the site of infection instead, which was more relevant to the treatment of pneumonia. This approach also circumvented the complexity of minocycline serum protein binding. We expected that the findings could be translated clinically, and then be used to optimize dosing regimen of minocycline. In future, this PK/PD model could provide rationale of minocycline dosing regimen design

for MDR *A. baumannii*. Using antibiotics correctly will considerably improve the success rate of treatment, and then reduce mortality of infections.

Although the minocycline resistance mechanisms in *A. baumannii* have been well studied, the information about how the resistance developed *in vivo* is unavailable. The resistant mutant of *A. baumannii* collected in our study could be a good tool for studying *in vivo* resistance development. It was derived from the wild type isolate (AB BAA 747), which exposed to minocycline in a neutropenic murine pneumonia model. The clonal relatedness between the mutants and AB BAA 747 has been confirmed. In future, the mutant gene(s) could be identified by whole genome sequencing. In addition to the currently known resistance mechanisms, this approach could also help discovering the potential unknown mechanism(s). Such information is expected to provide solutions for suppressing minocycline resistance development in *A. baumannii*.

REFERENCES

1. **Ventola C. L.** 2015. The antibiotic resistance crisis: part 1: causes and threats. P T **40:**277-283.

2. **Centers for Disease Control and Prevention.** 2017. Antibiotic / Antimicrobial Resistance https://www.cdc.gov/drugresistance/index.html. Accessed 07/12/2017.

3. **Smith R., Coast J.** 2013. The true cost of antimicrobial resistance. BMJ **346:**f1493.

4. **Centers for Disease Control and Prevention.** 2013. Antibiotic resistance threats in the United States. http://www.cdc.gov/drugresistance/threat-report-2013/pdf/ar-threats-2013-508.pdf. Accessed 03/21/2017.

5. **Lee C. R., Lee J. H., Park M., Park K. S., Bae I. K., Kim Y. B., Cha C. J., Jeong B. C., Lee S. H.** 2017. Biology of Acinetobacter baumannii: Pathogenesis, Antibiotic Resistance Mechanisms, and Prospective Treatment Options. Front Cell Infect Microbiol **7:**55.

6. **Gonzalez-Villoria A. M., Valverde-Garduno V.** 2016. Antibiotic-Resistant Acinetobacter baumannii Increasing Success Remains a Challenge as a Nosocomial Pathogen. J Pathog **2016:**7318075.

7. **Keen E. F., 3rd, Murray C. K., Robinson B. J., Hospenthal D. R., Co E. M., Aldous W. K.** 2010. Changes in the incidences of multidrug-resistant and extensively drug-resistant organisms isolated in a military medical center. Infect Control Hosp Epidemiol **31:**728-732.

8. **Abbo A., Carmeli Y., Navon-Venezia S., Siegman-Igra Y., Schwaber M. J.** 2007. Impact of multi-drug-resistant Acinetobacter baumannii on clinical outcomes. Eur J Clin Microbiol Infect Dis **26:**793-800.

9. **Zheng Y. L., Wan Y. F., Zhou L. Y., Ye M. L., Liu S., Xu C. Q., He Y. Q., Chen J. H.** 2013. Risk factors and mortality of patients with nosocomial carbapenem-resistant Acinetobacter baumannii pneumonia. Am J Infect Control **41:**e59-63.

10. **Denys G. A., Callister S. M., Dowzicky M. J.** 2013. Antimicrobial susceptibility among gram-negative isolates collected in the USA between

2005 and 2011 as part of the Tigecycline Evaluation and Surveillance Trial (T.E.S.T.). Ann Clin Microbiol Antimicrob **12:**24.

11. **Llor C., Bjerrum L.** 2014. Antimicrobial resistance: risk associated with antibiotic overuse and initiatives to reduce the problem. Ther Adv Drug Saf **5:**229-241.

12. **Fluit A. C., Florijn A., Verhoef J., Milatovic D.** 2005. Presence of tetracycline resistance determinants and susceptibility to tigecycline and minocycline. Antimicrob Agents Chemother **49:**1636-1638.

13. **Ribera A., Ruiz J., Vila J.** 2003. Presence of the Tet M determinant in a clinical isolate of Acinetobacter baumannii. Antimicrob Agents Chemother **47:**2310-2312.

14. **Speer B. S., Shoemaker N. B., Salyers A. A.** 1992. Bacterial resistance to tetracycline: mechanisms, transfer, and clinical significance. Clin Microbiol Rev **5:**387-399.

15. **Magnet S., Courvalin P., Lambert T.** 2001. Resistance-nodulation-cell division-type efflux pump involved in aminoglycoside resistance in Acinetobacter baumannii strain BM4454. Antimicrob Agents Chemother **45:**3375-3380.

16. **Damier-Piolle L., Magnet S., Bremont S., Lambert T., Courvalin P.** 2008. AdeIJK, a resistance-nodulation-cell division pump effluxing multiple antibiotics in Acinetobacter baumannii. Antimicrob Agents Chemother **52:**557-562.

17. **Hornsey M., Loman N., Wareham D. W., Ellington M. J., Pallen M. J., Turton J. F., Underwood A., Gaulton T., Thomas C. P., Doumith M., Livermore D. M., Woodford N.** 2011. Whole-genome comparison of two Acinetobacter baumannii isolates from a single patient, where resistance developed during tigecycline therapy. J Antimicrob Chemother **66:**1499-1503.

18. **Agwuh K. N., MacGowan A.** 2006. Pharmacokinetics and pharmacodynamics of the tetracyclines including glycylcyclines. J Antimicrob Chemother **58:**256-265.

19. **Watanabe A., Anzai Y., Niitsuma K., Saito M., Yanase K., Nakamura M.** 2001. Penetration of minocycline hydrochloride into lung tissue and sputum. Chemotherapy **47:**1-9.

20. **Goff D. A., Bauer K. A., Mangino J. E.** 2014. Bad bugs need old drugs: a stewardship program's evaluation of minocycline for multidrug-resistant Acinetobacter baumannii infections. Clin Infect Dis **59 Suppl 6:**S381-387.

21. **Casha S., Zygun D., McGowan M. D., Bains I., Yong V. W., Hurlbert R. J.** 2012. Results of a phase II placebo-controlled randomized trial of minocycline in acute spinal cord injury. Brain **135:**1224-1236.

22. **Nagpal K., Singh S. K., Mishra D. N.** 2013. Formulation, optimization, in vivo pharmacokinetic, behavioral and biochemical estimations of minocycline loaded chitosan nanoparticles for enhanced brain uptake. Chem Pharm Bull (Tokyo) **61:**258-272.

23. **Macdonald H., Kelly R. G., Allen E. S., Noble J. F., Kanegis L. A.** 1973. Pharmacokinetic studies on minocycline in man. Clin Pharmacol Ther **14:**852-861.

24. **Vella-Brincat J. W., Begg E. J., Kirkpatrick C. M., Zhang M., Chambers S. T., Gallagher K.** 2007. Protein binding of cefazolin is saturable in vivo both between and within patients. Br J Clin Pharmacol **63:**753-757.

25. **Dudley M. N., Shyu W. C., Nightingale C. H., Quintiliani R.** 1986. Effect of saturable serum protein binding on the pharmacokinetics of unbound cefonicid in humans. Antimicrob Agents Chemother **30:**565-569.

26. **Mukker J. K., Singh R. P., Derendorf H.** 2014. Determination of atypical nonlinear plasma-protein-binding behavior of tigecycline using an in vitro microdialysis technique. J Pharm Sci **103:**1013-1019.

27. **Thabit A. K., Monogue M. L., Nicolau D. P.** 2016. Eravacycline Pharmacokinetics and Challenges in Defining Humanized Exposure In Vivo. Antimicrob Agents Chemother **60:**5072-5075.

28. **Muralidharan G., Micalizzi M., Speth J., Raible D., Troy S.** 2005. Pharmacokinetics of tigecycline after single and multiple doses in healthy subjects. Antimicrob Agents Chemother **49:**220-229.

29. **Singh R. S., Mukker J. K., Deitchman A. N., Drescher S. K., Derendorf H.** 2016. Role of Divalent Metal Ions in Atypical Nonlinear Plasma Protein Binding Behavior of Tigecycline. J Pharm Sci **105:**3409-3414.

30. **Passaro L., Harbarth S., Landelle C.** 2016. Prevention of hospital-acquired pneumonia in non-ventilated adult patients: a narrative review. Antimicrob Resist Infect Control **5:**43.

31. **Lux L. J., Posey R. E., Daniels L. S., Henke D. C., Durham C., Jonas D. E., Lohr K. N.** 2014. Pharmacokinetic/Pharmacodynamic Measures for Guiding Antibiotic Treatment for Hospital-Acquired Pneumonia, Rockville (MD).

32. **Montravers P., Harpan A., Guivarch E.** 2016. Current and Future Considerations for the Treatment of Hospital-Acquired Pneumonia. Adv Ther **33:**151-166.

33. **Kalil A. C., Metersky M. L., Klompas M., Muscedere J., Sweeney D. A., Palmer L. B., Napolitano L. M., O'Grady N. P., Bartlett J. G., Carratala J., El Solh A. A., Ewig S., Fey P. D., File T. M., Jr., Restrepo M. I., Roberts J. A., Waterer G. W., Cruse P., Knight S. L., Brozek J. L.** 2016. Management of Adults With Hospital-acquired and Ventilator-associated Pneumonia: 2016 Clinical Practice Guidelines by the Infectious Diseases Society of America and the American Thoracic Society. Clin Infect Dis **63:**e61-e111.

34. **Vincent J. L., Rello J., Marshall J., Silva E., Anzueto A., Martin C. D., Moreno R., Lipman J., Gomersall C., Sakr Y., Reinhart K., Investigators Epic Ii Group of.** 2009. International study of the prevalence and outcomes of infection in intensive care units. JAMA **302:**2323-2329.

35. **Bowers D. R., Cao H., Zhou J., Ledesma K. R., Sun D., Lomovskaya O., Tam V. H.** 2015. Assessment of minocycline and polymyxin B combination against Acinetobacter baumannii. Antimicrob Agents Chemother **59:**2720-2725.

36. **Yuan Z., Ledesma K. R., Singh R., Hou J., Prince R. A., Tam V. H.** 2010. Quantitative assessment of combination antimicrobial therapy against multidrug-resistant bacteria in a murine pneumonia model. J Infect Dis **201:**889-897.

37. **World Health Organization.** 2014. Antimicrobial resistance: Global report on surveillance. http://www.who.int/drugresistance/documents/AMR_report_Web_slide_set.pdf Accessed 03/23/2017.

38. **Asin-Prieto E., Rodriguez-Gascon A., Isla A.** 2015. Applications of the pharmacokinetic/pharmacodynamic (PK/PD) analysis of antimicrobial agents. J Infect Chemother **21:**319-329.

39. **Zhou J., Ledesma K. R., Chang K. T., Abodakpi H., Gao S., Tam V. H.** 2017. Pharmacokinetics and pharmacodynamics of minocycline against Acinetobacter baumannii in a neutropenic murine pneumonia model. Antimicrob Agents Chemother doi:10.1128/AAC.02371-16.

40. **Lim T. P., Ledesma K. R., Chang K. T., Hou J. G., Kwa A. L., Nikolaou M., Quinn J. P., Prince R. A., Tam V. H.** 2008. Quantitative assessment of combination antimicrobial therapy against multidrug-resistant Acinetobacter baumannii. Antimicrob Agents Chemother **52:**2898-2904.

41. **Andersson D. I., Hughes D.** 2009. Gene amplification and adaptive evolution in bacteria. Annu Rev Genet **43:**167-195.

42. **Drlica K.** 2003. The mutant selection window and antimicrobial resistance. J Antimicrob Chemother **52:**11-17.

43. **Baquero F.** 1990. Resistance to quinolones in gram-negative microorganisms: mechanisms and prevention. Eur Urol **17 Suppl 1:**3-12.

44. **Drlica K., Zhao X.** 2007. Mutant selection window hypothesis updated. Clin Infect Dis **44:**681-688.

45. **Clinical and Laboratory Standards Institute.** 2012. Methods for Dilution Antimicrobial Susceptibilith Test for Bacteria Tht Grow Aerobically; Approved Stand-Ninth Edition. https://www.researchgate.net/file.PostFileLoader.html?id=56466b465f7f71946b8b45f2&assetKey=AS%3A295464181223441%401447455558839. Accessed 03/23/2017.

46. **Tam V. H., Ledesma K. R., Schilling A. N., Lim T. P., Yuan Z., Ghose R., Lewis R. E.** 2009. In vivo dynamics of carbapenem-resistant Pseudomonas aeruginosa selection after suboptimal dosing. Diagn Microbiol Infect Dis **64:**427-433.

47. **Monton C., Torres A., El-Ebiary M., Filella X., Xaubet A., de la Bellacasa J. P.** 1999. Cytokine expression in severe pneumonia: a bronchoalveolar lavage study. Crit Care Med **27:**1745-1753.

48. **Singh RSP, Falcao NMS, Sutcliffe J, Derendorf H.** 2013. Plasma Protein Binding of Eravacycline in Mouse, Rat, Rabbit, Cynomolgus Monkey, African Green Monkey and Human Using Microdialysis, abstr Interscience Conference on Antimicrobial Agents and Chemotherapy, Denver, CO,

49. **Abodakpi H., Gohlke J., Chang K. T., Chow D. S., Tam V. H.** 2015. Analytical and functional determination of polymyxin B protein binding in serum. Antimicrob Agents Chemother **59:**7121-7123.

50. **He J., Abdelraouf K., Ledesma K. R., Chow D. S., Tam V. H.** 2013. Pharmacokinetics and efficacy of liposomal polymyxin B in a murine pneumonia model. Int J Antimicrob Agents **42:**559-564.

51. **D'Argenio David Z., Schumitzky Alan, Wang Xiaoning.** 2009. ADAPT 5 User's Guide: Pharmacokinetic/Pharmacodynamic Systems Analysis Software. Los Angeles: Biomedical Simulations Resource, University of Southern California.

52. **Fish D. N., Chow A. T.** 1997. The clinical pharmacokinetics of levofloxacin. Clin Pharmacokinet **32:**101-119.

53. **Cortez-Cordova J., Kumar A.** 2011. Activity of the efflux pump inhibitor phenylalanine-arginine beta-naphthylamide against the AdeFGH pump of Acinetobacter baumannii. Int J Antimicrob Agents **37:**420-424.

54. **Tam V. H., Chang K. T., LaRocco M. T., Schilling A. N., McCauley S. K., Poole K., Garey K. W.** 2007. Prevalence, mechanisms, and risk factors of carbapenem resistance in bloodstream isolates of Pseudomonas aeruginosa. Diagn Microbiol Infect Dis **58:**309-314.

55. **Syrmis M. W., O'Carroll M. R., Sloots T. P., Coulter C., Wainwright C. E., Bell S. C., Nissen M. D.** 2004. Rapid genotyping of Pseudomonas aeruginosa isolates harboured by adult and paediatric patients with cystic fibrosis using repetitive-element-based PCR assays. J Med Microbiol **53:**1089-1096.

56. **Hirsch E. B., Guo B., Chang K. T., Cao H., Ledesma K. R., Singh M., Tam V. H.** 2013. Assessment of antimicrobial combinations for Klebsiella pneumoniae carbapenemase-producing K. pneumoniae. J Infect Dis **207:**786-793.

57. **Durmaz R., Otlu B., Koksal F., Hosoglu S., Ozturk R., Ersoy Y., Aktas E., Gursoy N. C., Caliskan A.** 2009. The optimization of a rapid pulsed-field gel electrophoresis protocol for the typing of Acinetobacter baumannii, Escherichia coli and Klebsiella spp. Jpn J Infect Dis **62:**372-377.

58. **Zeitlinger M. A., Derendorf H., Mouton J. W., Cars O., Craig W. A., Andes D., Theuretzbacher U.** 2011. Protein binding: do we ever learn? Antimicrob Agents Chemother **55:**3067-3074.

59. **Oravcova J., Bohs B., Lindner W.** 1996. Drug-protein binding sites. New trends in analytical and experimental methodology. J Chromatogr B Biomed Appl **677:**1-28.

60. **Scholtan W.** 1978. [Methods of determination and theoretical principles of the serum protein binding of drugs (author's transl)]. Arzneimittelforschung **28:**1037-1047.

61. **Herrera A. M., Scott D. O., Lunte C. E.** 1990. Microdialysis sampling for determination of plasma protein binding of drugs. Pharm Res **7:**1077-1081.

62. **Le Quellec A., Dupin S., Tufenkji A. E., Genissel P., Houin G.** 1994. Microdialysis: an alternative for in vitro and in vivo protein binding studies. Pharm Res **11:**835-838.

63. **Maia M. B., Saivin S., Chatelut E., Malmary M. F., Houin G.** 1996. In vitro and in vivo protein binding of methotrexate assessed by microdialysis. Int J Clin Pharmacol Ther **34:**335-341.

64. **Verbeeck R. K.** 2000. Blood microdialysis in pharmacokinetic and drug metabolism studies. Adv Drug Deliv Rev **45:**217-228.

65. **Saivin S., Houin G.** 1988. Clinical pharmacokinetics of doxycycline and minocycline. Clin Pharmacokinet **15:**355-366.

66. **Brogan T. D., Neale L., Ryley H. C., Davies B. H., Charles J.** 1977. The secretion of minocycline in sputum during therapy of bronchopulmonary infection in chronic chest diseases. J Antimicrob Chemother **3:**247-251.

67. **Jonas M., Cunha B. A.** 1982. Minocycline. Ther Drug Monit **4:**137-145.

68. **Nagata S., Yamashita S., Kurosawa M., Kuwajima M., Hobo S., Katayama Y., Anzai T.** 2010. Pharmacokinetics and tissue distribution of minocycline hydrochloride in horses. Am J Vet Res **71:**1062-1066.

69. **Schnabel L. V., Papich M. G., Divers T. J., Altier C., Aprea M. S., McCarrel T. M., Fortier L. A.** 2012. Pharmacokinetics and distribution of minocycline in mature horses after oral administration of multiple doses and comparison with minimum inhibitory concentrations. Equine Vet J **44:**453-458.

70. **Nelis H. J., De Leenheer A. P.** 1982. Metabolism of minocycline in humans. Drug Metab Dispos **10:**142-146.

71. **Bocker R. H., Peter R., Machbert G., Bauer W.** 1991. Identification and determination of the two principal metabolites of minocycline in humans. J Chromatogr **568:**363-374.

72. **Heaney D., Eknoyan G.** 1978. Minocycline and doxycycline kinetics in chronic renal failure. Clin Pharmacol Ther **24:**233-239.

73. **Sklenar I., Spring P., Dettli L.** 1977. One-dose and multiple-dose kinetics of minocycline in patients with renal disease. Agents Actions **7:**369-377.

74. **Tenover F. C., Arbeit R. D., Goering R. V., Mickelsen P. A., Murray B. E., Persing D. H., Swaminathan B.** 1995. Interpreting chromosomal DNA restriction patterns produced by pulsed-field gel electrophoresis: criteria for bacterial strain typing. J Clin Microbiol **33:**2233-2239.

75. **Izumiya H., Terajima J., Wada A., Inagaki Y., Itoh K. I., Tamura K., Watanabe H.** 1997. Molecular typing of enterohemorrhagic Escherichia coli O157:H7 isolates in Japan by using pulsed-field gel electrophoresis. J Clin Microbiol **35:**1675-1680.

76. **Murase T., Nakamura A., Matsushima A., Yamai S.** 1996. An epidemiological study of Salmonella enteritidis by pulsed-field gel electrophoresis (PFGE): several PFGE patterns observed in isolates from a food poisoning outbreak. Microbiol Immunol **40:**873-875.

77. **Murase T., Yamai S., Watanabe H.** 1999. Changes in pulsed-field gel electrophoresis patterns in clinical isolates of enterohemorrhagic Escherichia coli O157:H7 associated with loss of Shiga toxin genes. Curr Microbiol **38:**48-50.

78. **Yoshioka M., Kikuchi A., Matsumoto M., Ushiki T., Minami M., Saito H.** 1993. Evaluation of 5-hydroxytryptamine concentration in portal vein measured by microdialysis. Res Commun Chem Pathol Pharmacol **79:**370-376.

79. **Ofner B., Boukhabza A., Pacha W., Amsterdam C. V., Wintersteiger R.** 1997. Determination of SDZ ICM 567 in blood and muscle microdialysis samples by microbore liquid chromatography with ultraviolet and fluorescence detection. J Chromatogr B Biomed Sci Appl **700:**191-200.

80. **Rice C. J., Ramachandran V. K., Shearer N., Thompson A.** 2015. Transcriptional and Post-Transcriptional Modulation of SPI1 and SPI2 Expression by ppGpp, RpoS and DksA in Salmonella enterica sv Typhimurium. PLoS One **10:**e0127523.

81. **Karageorgopoulos D. E., Falagas M. E.** 2008. Current control and treatment of multidrug-resistant Acinetobacter baumannii infections. Lancet Infect Dis **8:**751-762.

82. **Yoon J., Urban C., Terzian C., Mariano N., Rahal J. J.** 2004. In vitro double and triple synergistic activities of Polymyxin B, imipenem, and rifampin against multidrug-resistant Acinetobacter baumannii. Antimicrob Agents Chemother **48:**753-757.

83. **Wareham D. W., Bean D. C., Khanna P., Hennessy E. M., Krahe D., Ely A., Millar M.** 2008. Bloodstream infection due to Acinetobacter spp: epidemiology, risk factors and impact of multi-drug resistance. Eur J Clin Microbiol Infect Dis **27:**607-612.

84. **Galani I., Orlandou K., Moraitou H., Petrikkos G., Souli M.** 2014. Colistin/daptomycin: an unconventional antimicrobial combination synergistic in vitro against multidrug-resistant Acinetobacter baumannii. Int J Antimicrob Agents **43:**370-374.

85. **Zhou J, Tam VH, Hu M.** 2015. A Rapid and Robust LC-MS/MS Method for Simultaneous Determination of Multiple Antibiotics in Human Serum, abstr American Association of Pharmaceutical Scientists, Denver,